4 Neutron diffraction studies on liquids

By G. W. NEILSON[a] and A. K. ADYA[b]

[a]*H. H. Wills Physics Laboratory, University of Bristol, Tyndall Avenue, Bristol BS8 1TL, UK*

[b]*Division of Applied Chemistry, School of Molecular and Life Sciences, University of Abertay Dundee, Bell Street, Dundee DD1 1HG, UK*

1 Introduction

The method of neutron diffraction is well suited to the study of liquid structure.[1] It has several advantages over other diffraction methods. These advantages are a direct consequence of the fact that neutrons interact mainly with the nuclei of the system *via* the strong nuclear force. As a result, the information contained in a diffraction pattern can be directly related to the internuclear (or interatomic) structure of the system. Neutrons are also only weakly absorbed by most materials, including iron, nickel, titanium, *etc*. Moreover, by mixing elements in the correct proportion one can fabricate so-called 'null' alloy containers which do not contribute to the structure contained in a diffraction pattern. As a result, one can easily fabricate pressure containers for work at elevated pressures and non-ambient temperatures. The most popular of these is an alloy of titanium and zirconium ($Ti_{0.68}Zr_{0.32}$) which has the strength of an intermediate steel and is relatively inert to corrosive attack. Finally, neutrons are coherently scattered equally strongly by light or heavy elements, *i.e*. hydrogen scatters just as effectively as manganese. In contrast to X-ray diffraction where X-rays are scattered more strongly by atoms with higher atomic number, there is no simple relationship between scattering 'power' and nucleus. As a result neutrons can be used to probe the structure of materials containing hydrogen, lithium, *etc*.

For complex liquid and amorphous systems the difference techniques of isotopic substitution can be used to determine structural details at high resolution.[2] For the past three decades, these methods have been used to elucidate the interatomic structure in a diversity of liquids ranging from simple fluids such as argon to complex biological materials such as aqueous solutions of DNA.

The main objective of neutron diffraction is the determination of structure in terms of the pair radial distribution functions, $g_{\alpha\beta}(r)$, of the system. It will be recalled that these functions are the first in a hierarchy of interatomic correlations; they are the only ones directly accessible from experiment and provide information on the local order around atoms in the liquid.[1] For a simple monatomic liquid such as argon, there is only one radial distribution function $g(r)$. Inspection of Fig. 1 shows how the local structure can be broken down into several parts such as contact distance, nearest neighbour distance, next nearest neighbour distance, *etc*., and eventually end of short-

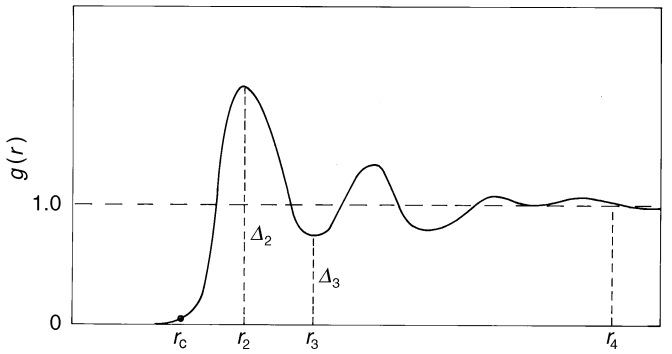

Fig. 1 A typical pair distribution function $g(r)$ for a liquid: r_c is the closest distance of approach of the two particles, r_2 the most probable nearest neighbour separation, r_3 the extent of the first coordination shell, r_4 the end of short range order and Δ_2/Δ_3 a measure of the degree of sharpness (or stability) of the first coordination shell.

range order. Additionally by an examination of the shapes of the correlations in $g(r)$, one can obtain a qualitative guide to the degree of complexation. For example, in molecular liquids and electrolyte solutions it is often observed that molecular units or pseudo molecular complexes are evident in the experimentally determined radial distribution functions (Fig. 2–10).

For a binary mixture (A_xB_{1-x}), a diatomic molecular liquid or simple molten salt, AB_n, there are three pair functions $g_{AA}(r)$, $g_{BB}(r)$ and $g_{AB}(r)$. As the number of independent species, m, increases, so the number of pair functions scales according to the rule $m(m+1)/2$, and for a system with three or four distinct atomic species there are six and ten $g_{\alpha\beta}(r)$ values, respectively. The number of $g_{\alpha\beta}(r)$ becomes proportionally greater in more complex systems. A knowledge of the $g_{\alpha\beta}(r)$ values enables us to characterise the local structure of the liquid and also provides a useful test of models used in computer simulation studies.

The difference methods of neutron diffraction and isotopic substitution (NDIS) are ideally suited to the determination of these functions individually or as linear combinations of the form $G_\alpha(r)$, which is specific to the substituted species α. The usefulness of this approach can readily be illustrated by reference to an aqueous electrolyte solution of a salt (MX_n) in water (H_2O).[3] The first difference method applied to cations or anions by isotopic exchange of M′ for M or X′ for X can be used to obtain information concerning aqua-ion structure in terms of the function $G_M(r)$ or $G_X(r)$. In mathematical terms

$$G_M(r) = Ag_{MO}(r) + Bg_{MH}(r) + Cg_{MX}(r) + Dg_{MM}(r) + E \quad (1)$$

where $A = 2c_Mc_Ob_O\Delta b_M$, $B = 2c_Mc_Hb_H\Delta b_M$, $C = 2c_Mc_Xb_X\Delta b_M$, $D = c_M^2[b_M^2 - (b'_M)^2]$, $\Delta b_M = b_M - b'_M$ and c_α is the atomic concentration of species α whose neutron coherent scattering length is b_α. By extension it can be shown that a second difference experiment involving isotopic exchanges of M′ for M, X′ for X, and deuterium (D) for hydrogen (H), can be used to obtain the individual pair functions for the solute [$g_{MM}(r)$,

$g_{MX}(r)$, $g_{XX}(r)$] and the solvent [$g_{HH}(r)$, $g^{*}_{OH}(r)$]. Note that the asterisk on $g_{OH}(r)$ means that it is only an approximation to the true $g_{OH}(r)$. However, in the limit of high dilution it will tend to the exact function as in pure water. It is also worth noting that because the scattering length of the oxygen isotopes ^{16}O, ^{17}O and ^{18}O are almost the same, determination of $g_{OO}(r)$ in pure water is liable to large errors, and is not yet accessible in solution.

The coordination number of α atoms around β is defined for the range $r_1 \leq r/\text{Å} \leq r_2$ as

$$\tilde{n}^{\alpha}_{\beta} = 4\pi c_{\alpha}\rho \int_{r_1}^{r_2} g_{\alpha\beta}(r) r^2 \mathrm{d}r \tag{2}$$

where ρ is the total number density in Å^{-3}. A hydration number for an ion I in solution can be defined as

$$\tilde{n}_{I}^{H_2O} = 4\pi\rho c_{O} \int_{r_1}^{r_2} g_{IO}(r) r^2 \mathrm{d}r \tag{2a}$$

or

$$\tilde{n}_{I}^{H_2O} = 4\pi\rho c_{H} \int_{r_1}^{r_2} g_{IH}(r) r^2 \mathrm{d}r \tag{2b}$$

depending which of these functions can be more readily identified. For more complex systems NDIS methods can again be used to isolate structure around a particular species or to determine individual radial distribution functions (rdf's). This procedure has been used successfully to determine the structure of molecular liquids and their mixtures, molten salts, liquid metals, aqueous solutions of large molecules, aqueous solutions of electrolytes and polyelectrolytes, and amorphous materials.

The success of NDIS experiments depends crucially on several factors. These include (i) high quality samples whose composition is accurately known in terms of atomic concentration and isotope content, (ii) a high flux neutron source which can provide sufficient statistical accuracy in the data, and (iii) stable instrumentation so that data are highly reproducible during the course of an experiment which takes typically *ca.* 10 h per sample. Results of NDIS experiments can be usefully compared with information on structure obtained from other methods. The closest of these to the neutron diffraction methods are X-ray diffraction,[4] EXAFS[5] and anomalous X-ray scattering.[6] The first of these is usually easier to apply and until the use of NDIS became widespread it was the only means used to determine liquid structure. EXAFS on the other hand is atom specific and useful results can be obtained especially as regards atom–atom distances, although coordination numbers may be less reliable because of the need to fit the spectroscopic EXAFS data over a limited range of momentum transfer. Anomalous scattering offers a truly competitive technique to NDIS and one looks forward to its application with optimism. Unfortunately it is limited to elements with an atomic number greater than *ca.* 25.

NDIS methods can also assist in the analysis of spectroscopic (*e.g.* Raman or

infrared) data which are targeted at the identification of chemical species in a liquid. However, if these species are short-lived and not dominant, they will not be detected by NDIS because $g_{\alpha\beta}(r)$ are average functions over all possible configurations and do not contain any information on individual species other than those which are long-lived and exhibit high degrees of correlation, *e.g.* the aqua-cation ($Ni^{2+} \cdots 6H_2O$). To obtain neutron based information which is equivalent to that obtained by one of the optical spectroscopies, one would use inelastic neutron scattering, the analysis of which is often complicated by an absence of selection rules when a neutron is absorbed or emitted in a collision with a nucleus of the liquid.

The information obtained in an NDIS experiment can provide a critical test of model potentials[7] and liquid state theories.[8] In contrast to X-ray scattering methods, the $g_{\alpha\beta}(r)$ and $G_\alpha(r)$ functions can be compared directly with the theoretical functions as they involve a mathematically proper Fourier transformation of the experimentally corrected data.

2 Results

The results presented below are necessarily limited to those liquids of most interest to the chemical community. Consequently simple liquids and quantum liquids are not discussed. There are excellent reviews on both topics: for the case of simple liquids the reader is referred to the new edition of the book by Egelstaff[1] and for quantum liquids the book by Glyde[9] gives an up-to-date account.

Nor will we discuss liquid metals, binary alloys, liquid semiconductors and glasses of these materials. For these systems the reader is referred to the work of Enderby and Barnes[10] and Elliot.[11] In the subsequent text we review results of neutron diffraction studies on a variety of systems, starting with molecular fluids and moving to systems of increasing complexity. Besides the results which are published in the literature, a rich source of additional information is also available in the form of the Annual Reports of the various Neutron Facilities, *e.g.* ISIS at Rutherford Appleton Laboratory, Chilton, UK; ILL, Grenoble, France; KENS at the KEK Facility in Tsukuba, Japan; *etc.* These publications contain progress reports on the status of experiments and describe state-of-the-art methods being used to tackle many topical problems concerning the atomic and molecular properties of soft matter.

Molecular liquids

Molecular liquids are, in general, more complex than atomic or ionic liquids and this complexity stems from two main factors. Firstly, the basic entities, the molecules, are not rigid: they have internal vibrations, and it is not a trivial problem to characterise them purely in terms of correlations of atomic positions. In reality, severe distortions from arrangements of highest symmetry of atomic positions over and above those arising from internal vibrations may be expected. However, in order to explore the intermolecular structure the molecules are assumed in many cases to be almost rigid and their geometry is usually taken from solid or gaseous state studies. Such an approach may be adequate for relatively small molecules but complications are bound to set in for larger molecules. In addition, for more complex molecules, various conformers may exist in solution. Secondly, the relative orientation of molecules in a molecular liquid is distinct from their centre–centre separations, and one must take

into account the orientational correlation in addition to the correlation between the molecular centres. Also, orientational correlations are expected to be strongly dependent on the separation of the molecules at closer distances while at larger separations there may exist no correlation of orientations. Obviously, a single scattering experiment cannot reveal all orientational correlations.

The neutron scattering pattern of a molecular liquid is usually more difficult to interpret than from an atomic/ionic liquid.[1] In general it consists of an unresolvable sum of several scattering patterns and becomes more complicated when the same type of nucleus is present in more than one position in the molecule (*e.g.* HCOOH). These difficulties can be overcome by the NDIS technique, but in view of the limited number of isotopic substitutions possible in molecular liquids, its use has been severely restricted; to date amongst the heavier elements only nitrogen and chlorine have been used successfully for isotopic substitution. Problems due to inelasticity effects and large incoherent scattering of hydrogen nuclei have until recently excluded the use of H/D substitutions. During the past decade H/D substitution has become feasible with the construction of specially designed diffractometers such as SANDALS at ISIS and with the introduction of more refined data analysis. The use of carbon in NDIS experiments has yet to be demonstrated; the difference in scattering lengths[12] of ^{12}C and ^{113}C is too small to provide quantitative information with present-day technology.

Even if it were possible to extract all the pair distribution functions [$g(r)$] in a molecular liquid, it is not clear that this would provide deeper physical insight of the system. Even for the simplest of molecular liquids the situation is considerably more complicated than that of non-atomic liquids because of the additional degrees of freedom introduced by the relative orientations of the molecules. While a pair correlation function $g(r)$ describing the correlation between atoms is a function of a single variable r, a similar function for molecular liquids is dependent on six variables: a separation vector r between the two molecules, two angles θ_1 and θ_2 to point the direction of the second molecule, and the three Euler angles α, β and γ to describe the relative orientation between the two molecules. For homonuclear diatomic molecules, owing to their symmetry, this number is reduced to four. There is thus a clear-cut limitation on the amount of information that can be obtained from a single diffraction experiment on a molecular liquid, and there is no way to map one-dimensional diffraction data onto a four- or six-dimensional function. Indeed, whatever information has been derived is at best semi-quantitative.

Inevitably one has almost always to resort to different kinds of models to describe the structure of a molecular liquid, and the validity of such models in the first place is judged by their ability to fit the experimentally determined structure. For this, the description of various liquids through structural models *via* computer simulations[14–20] such as molecular dynamics (MD) and statistical mechanical calculations,[21–23] for example, reference interaction site model 'RISM',[24,25] are compared with experimental results obtained from neutron diffraction (ND).[26–29] Diffraction data of high precision are necessary to characterise the positional and orientational correlations in molecular liquids. Since models are not unique, proliferation of spurious models in the literature can be avoided by fitting other known facts about the liquid, such as its atomic and molecular dynamics. However, this approach seems to have hardly been attempted.

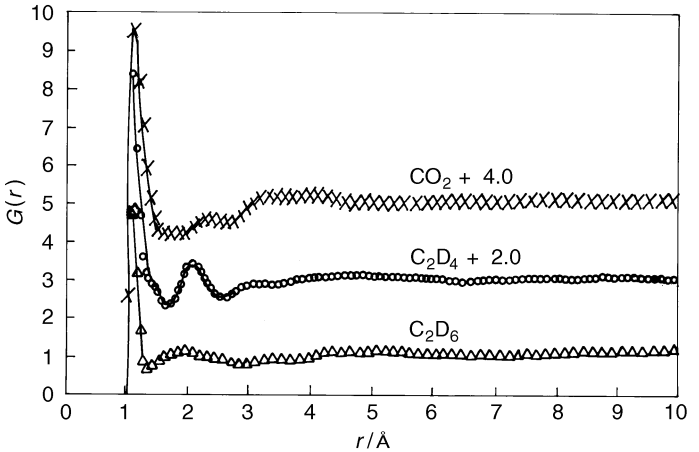

Fig. 2 The total distribution function $G(r)$ for the three molecular liquids, carbon dioxide, ethylene (C_2D_4) and ethane (C_2D_6).[37] Note the intramolecular contributions at low r.

Results from diffraction experiments performed over a number of thermodynamic states can provide a severe test of the applied theories and model potentials.[23–25,30–32] A significant change in the thermodynamic state of a liquid can be produced by varying its density through temperature (T) and pressure (p) variations. Such (p,T)-studies are also required if one wishes to disentangle the competing effects of temperature and density on liquid structure.[28,33,34]

In terms of formalism, the Faber–Ziman approach[13] used in atomic liquids, ionic liquids and solutions[1] is inappropriate for molecular systems. Instead an approach is employed which separates the structure into two parts: that of the molecules themselves or the intramolecular structure, and that of the correlations between molecules or the intermolecular structure.[1,35,36] The analysis of the neutron diffraction results is carried out in both the momentum transfer (Q) space of the experimental data, and in Fourier transform or real-space, r. The total structure pattern, $G(r)$ for the liquid contains both intra- and inter-molecular structure. For example, the liquid structures of carbon dioxide (CO_2), ethane (C_2D_6) and ethylene (C_2D_4) are shown in Fig. 2.[37] For CO_2(l), the $G(r)$ shows two intramolecular peaks occurring at 1.16 and 2.32 Å which correspond to the C–O and O–O distances in the molecule. Two more peaks appearing at about 3.3 and 4 Å in $G(r)$ for CO_2 arise due to contributions from intermolecular C–C, C–O and O–O distances and these peaks are well separated from the intramolecular ones. However, for C_2D_4(l) and C_2D_6(l), since the largest intramolecular distances are larger than the shortest intermolecular distances, it is not possible to separate the intra- and inter-molecular contributions by direct Fourier transformation of the experimental data.

To extract more information, one uses the data for the intramolecular structure contained in $G(r)$, to calculate an intramolecular form factor which is subtracted from the Q-space structural data. The resulting intermolecular scattering function is then

analysed to establish the type and extent of correlations between molecules.[35,38–41] At this stage the information can be compared with results from particular model calculations.

In a review of this size it is inappropriate to give a detailed account of each system studied. Instead we tabulate (Table 1) the various molecular liquids that have been studied to date by neutron diffraction, and discuss a few systems in detail.

A comprehensive review on structural studies of both homo- and hetero-nuclear diatomic and pseudo-diatomic molecular fluids has been published in 1991 by Andreani *et al.*;[167] the systems covered are D_2, N_2, O_2, F_2, Cl_2, Br_2, I_2, H/DF, H/DCl, DBr, CO, NO, CS_2, CSe_2 and CO_2. The neutron diffraction results of simple homonuclear diatomic liquids N_2, O_2 and F_2 do not show any asymmetry or broadening of the first peak in the intermolecular scattering function in contrast to those for heavy halogens (Cl_2, Br_2 and I_2) which show a marked broadening and asymmetry of this first peak. Such features are representative of correlations in the orientations of neighbouring molecules[23] in these liquids. Accordingly, homonuclear diatomic molecular liquids can be divided into two classes: one comprising N_2, O_2 and F_2 liquids without orientational correlations and the second comprising the heavy halogens which show strong orientational correlations. Application of the reverse Monte Carlo (RMC) technique[168] to the available diffraction data on the liquid halogens and nitrogen suggests that orientational correlations are largely confined to the nearest-neighbour coordination shell. The results also indicate an increased tendency for the neighbouring molecules in the heavier halogens to be aligned end-to-end; these observations are in contrast to what would be expected from purely quadrupole interactions. Although discrepancies between the simulation and experimental data on liquid halogens are still present, computer simulations by Rodger, Stone and Tildesley (RST),[20] which employ *ab initio* methods to evaluate the anisotropic interaction potential, give a reasonable explanation of the liquid behaviour without involving the quadrupole formalism. Thus, while systems such as liquid N_2, O_2, F_2 and CO are found to have a relatively simple behaviour, liquid halogens are only now beginning to be understood. The hydrogen bonded liquids (HF, HCl and HBr) continue to pose many problems which are yet to be resolved.

Since the publication of the review[167] on diatomic and some triatomic liquids, many new results have appeared in the literature. For example, Filabozzi *et al.*[70] have carried out a new determination of liquid bromine structure by ND and report that some discrepancies between their data and MD results based on the RST model[20] are still present.

The triatomic system CO_2 has been extensively studied over many thermodynamic states from near its triple point to above its critical point. Initial ND results[26,33,37] showed the existence of orientationally correlated molecules in CO_2 near its triple point at a very short range, and for modelling this system, it is only necessary to consider 'orientational correlations, in nearest neighbours. The structure beyond this region is probably a consequence of packing of uncorrelated molecules. Subsequent and more detailed investigations confirm these observations over a wider range of thermodynamic phase.[28,34,85,86] On the other hand, RISM calculations reveal that some structural features of both the liquid and supercritical fluid cannot be reproduced by any of the interaction potentials considered, thus indicating a deficiency in either the applied interaction potentials or the theory.[28,33,37]

Table 1 Molecular liquids/fluids and liquid/fluid mixtures investigated by the technique of neutron diffraction (ND) or with isotopic substitution (NDIS)

system	*ref.*
molecular liquids/fluids	
diatomics (homonuclear)	
D_2 (deuterium)	42–44
N_2 (nitrogen)	45–55
O_2 (oxygen)	45,46,50,51,54
F_2 (fluorine)	56
Cl_2 (chlorine)	41,57–61
Br_2 (bromine)	39,62–70
I_2 (iodine)	40,71,72
diatomics (heteronuclear)	
HF/DF (hydrogen fluoride)	73
HCl/DCl (hydrogen chloride)	27,74–78
HBr/DBr (hydrogen bromide)	79,80
HI (hydrogen iodide)	81,82
CO (carbon monoxide)	83,84
NO (nitric oxide)	83
triatomics	
CO_2 (carbon dioxide)	26,28,33,34,37,85,86
CS_2 (carbon disulfide)	87–89
CSe_2 (carbon diselenide)	87
H_2S (hydrogen sulfide)	90
SO_2 (sulfur dioxide)	91
alkanes and alkenes	
CH_4/CD_4 (methane)	29
C_2H_6/C_2D_6 (ethane)	37
C_2H_4/C_2D_4 (ethylene)	37
C_3D_6 (cyclopropane)	92–94
C_4D_{10} (*n*-butane)	95
C_6D_{12} (cyclohexane)	96,97
aromatics	
C_6H_6 (benzene)	98–101
$C_6H_5CH_3$ (toluene)	102
$C_6H_5NO_2$ (nitrobenzene)	102
$C_{10}H_8$ (naphthalene)	103
fluorinated compounds	
$CHClF_2$ (chlorofluoromethane)	104
CCl_2F_2 (dichlorodifluoromethane)	104,105
CHF_3 (fluoroform)	104
$C_6H_3F_3$ (1,3,5-trifluorobenzene)	106
C_6F_6 (hexafluorobenzene)	98
SF_6 (sulfur hexafluoride)	29

Table 1 (*cont.*)

system	*ref.*
other halogenated compounds	
CH_2Cl_2 (methylene chloride)	107
$CHCl_3$ (chloroform)	108–113
CCl_4 (carbon tetrachloride)	38,114–118
$C_2H_4Cl_2$ (1,2-dichloroethane)	119,120
C_3H_7Cl (2-chloropropane)	121
C_3H_7Br (2-bromopropane)	121
C_6H_5Br (bromobenzene)	102,122,123
$SiCl_4$ (silicon tetrachloride)	114,115
$TiCl_4$ (titanium tetrachloride)	114,115
$VOCl_3$ (vanadium oxytrichloride)	124
VCl_4 (vanadium tetrachloride)	114,124
$GeCl_4$ (germanium tetrachloride)	114,115
$GeBr_4$ (germanium tetrabromide)	114
$SnCl_4$ (tin tetrachloride)	114,115
alcohols and ketones	
CH_3OH (methanol)	125–133
C_2D_5OD (ethanol)	134,135
C_3H_7OH (propan-2-ol)	136,137
$C_3H_8O_3$ (D-glycerol)	138
C_3H_6O (acetone)	139,140
acids	
DCOOD (formic acid)	141–143
CH_3COOH (acetic acid)	144
miscellaneous	
NH_3 (ammonia)	145–148
PBr_3 (phosphorus tribromide)	149,150
C_2O_3 (carbon suboxide)	151
$HCONH_2$ (formamide)	152, 153
C_2H_5NO (*N*-methylformamide)	154
CH_3CN (acetonitrile)	155, 156
C_5H_5N (pyridine)	157
$(CH_3)_2SO$ (dimethyl sulfoxide, DMSO)	158–160
liquid mixtures	
$CO_2 + C_2D_4$ (carbon dioxide + ethylene)	161
$CO_2 + C_2D_6$ (carbon dioxide + ethane)	161
$CS_2 + CCl_4$ (carbon disulfide + carbon tetrachloride)	162
$C_6H_6 + C_6F_6$ (benzene + hexafluorobenzene)	163
$TiCl_4 + SiCl_4$ (titanium chloride + silicon tetrachloride)	164,165
$TiCl_4 + SnCl_4$ (titanium chloride + tin tetrachloride)	164,165
$(CH_3)_2SO + H_2O$ (DMSO + water)	166

Bausenwein *et al.*[27] performed ND measurements on DCl at seven thermodynamic states and observed a very small effect of temperature variation on its structure. The effect of density variation was found to be more significant. The authors also succeeded in determining a potential capable of reproducing experimental results for different thermodynamic states. ND measurements on liquid ammonia at four different densities have been reported by Bertagnolli *et al.*[148] The authors were unable to detect the presence of any hydrogen bond in liquid ammonia. They tested a series of potentials and were able to obtain one which could reproduce the experimental data.

Strauss *et al.*[29] have performed ND measurements on spherical molecules such as CH_4 and SF_6 by varying their densities at supercritical temperatures. A crystalline-like order observed for SF_6 at the highest density was found to vanish with a reduction in its density. However, the variation in density was found to have only a very weak effect on the intermolecular correlation function of CH_4. In both cases RISM calculations were also performed to deduce a suitable potential capable of reproducing the experimental data over the investigated thermodynamic states.

Adya and Wormald[37] reported the intra- and inter-molecular structure in the condensed phases of deuteriated ethylene, C_2D_4 and ethane, C_2D_6, and observed only a slight relaxation of the structure on melting. Quadrupole–quadrupole interactions were found to have a dominating role in determining the local structure of the two liquids.

Bartsch *et al.*[98] investigated the contribution of quadrupole–quadrupole interactions in the aromatic systems benzene and hexafluorobenzene where dispersion and induction interactions are expected to be weak, and found a dominating effect of electrostatic forces on the local structure of the two liquids. In order to determine whether packing effects or electrostatic effects are the structure determining factors in the presence of varying dipolar forces, ND experiments were carried out on three aromatic systems,[102] toluene, nitrobenzene and bromobenzene, having very similar sizes of the substituents on the benzene ring but with dipole moments significantly different.

Luzar *et al.*[159,160] combined NDIS and computer simulation techniques to study the structure of liquid dimethyl sulfoxide (DMSO) with a large dipole moment, and they suggest that both packing effects and the electrostatic interactions play a role in determining the structure of this liquid. However, their results indicate a lack of highly ordered molecular association in the liquid owing to the absence of highly specific and powerful forces such as hydrogen bonds in water or methanol. Bertagnolli *et al.*[158] combined X-ray and neutron diffraction and found from their cluster calculations that the local order in liquid DMSO is similar to that in its solid state.

Liquid mixtures

Unfortunately only a few liquid mixtures have been investigated by the technique of neutron diffraction (Table 1). This situation is undoubtedly due to increased difficulty in the interpretation of the diffraction data.

Adya and Wormald[161] performed ND experiments on equimolar liquid mixtures $CO_2 + C_2D_4$ and $CO_2 + C_2D_6$, and also on their pure components. The three molecules are of similar size and shape. The critical temperatures of the three fluids are similar and the liquids are miscible in all proportions. The major difference between the two mixtures is in the sign of the quadrupole moments of the unlike molecules. As

the quadrupole moments of CO_2 and C_2H_6 are of the same sign it is expected that the quadrupole coupling will be weak. The quadrupole moments of CO_2 and C_2H_4 are of opposite sign, and strong quadrupole coupling is expected to orientate the molecules. The thermodynamic behaviour of the two liquid mixtures is quite different in that $CO_2 + C_2H_6$ has a positive azeotrope while $CO_2 + C_2H_4$ has a negative azeotrope, and this difference in behaviour is thought to be due to different quadrupole forces between the unlike molecules. Adya and Wormald[161] conclusively demonstrated from their ND results that electrostatic quadrupole interactions play a significant role in determining the local structure of the two liquid mixtures. The results were found to be consistent with a nearly parallel orientation or stacking of CO_2 and C_2D_4 molecules in the equimolar mixture, which is the most stable geometry for quadrupolar molecules of opposite sign.[169] However, for $CO_2 + C_2D_6$, where the component molecules have quadrupole moments of the same sign, the results indicate a nearly perpendicular or L-shaped geometry for the unlike molecules in this mixture.

In another study, Bartsch *et al.*[163] combined neutron and X-ray diffraction measurements on liquid benzene–hexafluorobenzene mixtures at three compositions along with those on their pure components to determine whether packing effects or electrostatic interactions are the structure-determining factors. The authors concluded that the quadrupole interaction is the structure determining factor in the investigated liquid aromatic systems. Through a combined analysis of the neutron and X-ray data they showed that a reorientation takes place from a L-type pair geometry in the pure components to a nearly parallel alignment of the molecules in the equimolar mixture as is expected for quadrupoles of opposite sign.

The methods of ND and NDIS will continue to play a significant role in deepening our understanding of molecular liquids and their mixtures, by providing quantitative structural information which can be used to examine critically model-based simulations and liquid state theories.

Molten salts

Molten salts are predominantly Coulombic type liquids, with physical properties closely related to their ionic liquid structure. Detailed and unique structural information about the short-range chemical order in liquid melts containing more than one chemical species can be obtained from NDIS methods. Page and Mika were the first to apply the NDIS technique[170] to the structural study of molten CuCl.[171] Subsequently, Edwards *et al.*[172] applied this technique to the 1:1 molten halide salts and then also to 2:1 halide melts[173] followed by other investigators in the field. This work was extended by Howe *et al.*[174] to the studies of molten halide mixtures. Among others, Adya and Neilson[175–177] applied this technique to pure and mixed molten nitrates. Adya and Takagi *et al.*[178] have recently initiated investigations into lanthanide halides and their mixtures with alkali halides. Theorists have not lagged behind and numerous computer simulations of the molten salt systems have been performed.[179–192] With current interest in powerful X-ray sources such as the European Synchrotron Source (ESF) at Grenoble and the Photon Factory at Argonne National Laboratory, emphasis is now being focused on the complementary use of X-ray and neutron scattering methods. This can overcome the need to acquire expensive isotopes and enables a study to be made of materials whose isotopes have high absorption coefficients, large neutron resonances and relatively small contrast variations.

Table 2 Structural properties of molten alkali halides, and other 1:1 halides

molten salt	*technique/ (ref.)*	T/°C	r_{c+-} [a]	r_{+-}	n_{+-}	r_{s+-} [b]	r_{c--} [a]	r_{--}	n_{--}	r_{s--} [b]	r_{c++} [a]	r_{++}	n_{++}	r_{s++} [b]	$r_+/\AA$	r_{--}/r_{+-}
LiCl	NDIS (194)	685	—	2.3	3.5–4.0	2.41	—	3.7	—	3.62	—	3.7	—	1.2	0.60	1.61
LiCl	NDIS (196)	685	2.9	—	5.5	2.41	1.9	—	—	3.62	2.0	—	—	1.2	0.60	—
NaCl	NDIS (172)	875	2.09	2.72	5.8	2.76	3.19	3.9	13.3	3.62	3.19	3.89	13.0	1.9	0.95	1.43
NaCl	NDIS (198)	875	2.09	2.78	5.8	2.76	3.19	3.9	13.3	3.62	3.19	3.96	13.0	1.9	0.95	1.41
KCl	NDIS (200)	800	2.20	3.06	6.1	3.14	3.40	4.82	12.3	3.62	3.50	4.84	12	2.66	1.33	1.58
RbCl	NDIS (201)	750	2.7	3.18	6.9	3.29	3.6	4.8	14	3.62	3.55	4.86	13	2.96	1.48	1.5
CsCl	NDIS (202)	695	2.8	3.4	5.8	3.5	3.45	4.85	16.3	3.62	3.45	4.95	15.4	3.38	1.69	1.43
CsCl	NDIS (200)	700	2.45	3.38	—	3.5	3.40	3.85	—	3.62	3.40	3.85	—	3.38	1.69	—
CuCl	NDIS (203)	500	1.7	2.3	3	2.77	2.6	3.9	—	3.62	1.7	3.7	—	1.92	0.96	1.69
CuCl	NDIS (171)	440	2.0	2.3	—	2.77	3.0	3.6	—	3.62	1.5	3.3	—	1.92	0.96	1.57
CuBr	NDIS (205)	515	—	2.5	3.63	2.91	—	3.97	11.1	3.90	—	—	—	1.92	0.96	1.59
AgCl	NDIS (204)	510	1.8	2.6	4.3	—	2.6	—	—	3.62	2.5	3.4	3.1	—	—	—
AgCl	NDIS (204)	850	1.65	2.55	2.7	—	2.7	3.15	2.7	3.62	2.65	3.15	4.1	—	—	—

[a] r_c = closest distance of approach. [b] r_s = sum of ionic radii. r_{ij}'s are positions of the first maximum in the $g_{ij}(r)$'s and n_{ij}'s are nearest neighbour coordination numbers.

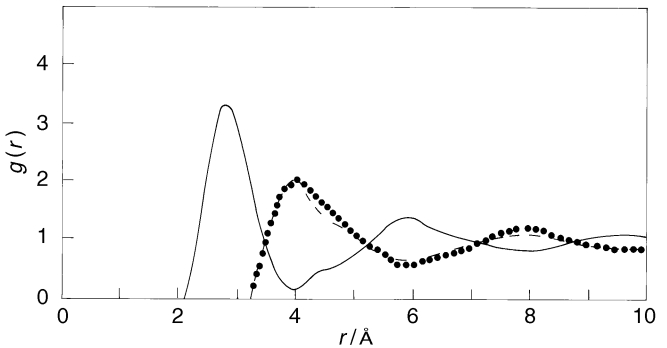

Fig. 3 The three radial pair distribution functions in molten sodium chloride at 1148 K:[198] $g_{NaNa}(r)$, dotted curve; $g_{ClCl}(r)$, dashed curve; $g_{NaCl}(r)$, full curve.

Molten alkali chlorides and other 1 : 1 chlorides

Because the two stable isotopes of chlorine (^{35}Cl and ^{37}Cl) have large differences in neutron scattering lengths,[193] it is perhaps not surprising that initial studies of molten salts were concerned with alkali chlorides and other molten metal chlorides.[171,172,194–205] Moreover, the molten alkali halides were amongst the first salts to be studied theoretically and by computer simulations.[179,180,184] The fact that NDIS methods could be used to determine $g_{++}(r)$, $g_{+-}(r)$ and $g_{--}(r)$ for a large number of systems provided theorists with a critical test of their potentials. Results for systems such as NaCl, LiCl, KCl, RbCl and CsCl are well documented (Table 2), and serve to illustrate the extent to which our knowledge of such systems has improved over the past 20 years (Fig. 3). It is now clear that for such systems theoretical models based on Fumi–Tosi potentials can adequately describe many of the structural features. However, one notices that as the size of the cation increases there is a need to include polarisation effects.

Recent work on CuCl by Eisenberg *et al.*,[203] which is generally similar though of higher accuracy than that of Page and Mika,[171] indicates that it is only weakly ionic, with a tendency to charge ordering at large distances. The coordination number for unlike atoms determined from the partial Cu–Cl radial distribution function in the melt is found to be 3 ± 0.7, which is lower than 4 found in solid γ-CuCl. The authors conclude that the weakness of ionicity combined with a small coordination number for the unlike atoms in the nearest neighbour shell and the relatively small size of copper atom seem to favour short Cu–Cu distances. By the same methods molten CuBr is shown[205] to possess a similar structure to CuCl; both melts show (i) a featureless cation–cation partial structure factor and distribution function, (ii) a considerable asymmetry between Cu–Cu and X–X pair distribution functions, and (iii) a large degree of first-shell penetration by the copper ions. While CuCl shows a three-fold coordination of Cl^- ions around Cu^+, CuBr shows a predominantly tetrahedral local environment of Br^- ions around Cu^+ (Table 2).

Table 3 Structural properties of molten 2:1 and 3:1 halides

molten salt	*technique/ (ref.)*	T/°C	r_{c+-} [a]	r_{+-}	n_{+-}	r_{s+-} [b]	r_{c--} [a]	r_{--}	n_{--}	r_{s--} [b]	r_{c++} [a]	r_{++}	n_{++}	r_{s++} [b]	r_+/Å	r_{--}/r_{+-}	$r_{prepeak}$/Å
$ZnCl_2$	NDIS (173)	327	1.9	2.29	4.3	2.55	3.0	3.71	8.6	3.62	2.8	3.8	4.7	1.48	0.74	1.62	1.03
$ZnCl_2$	ND (207)	330	—	2.29	3.93	2.55	—	3.79	—	3.62	—	—	—	1.48	0.74	1.65	1.005
$ZnCl_2$	ND (207)	600	—	2.31	3.67	2.55	—	3.86	—	3.62	—	—	—	1.48	0.74	1.67	0.944
$ZnBr_2$	ND (207)	420	—	2.42	3.9	2.69	—	4.08	—	3.9	—	—	—	1.48	0.74	1.68	0.943
ZnI_2	ND (207)	470	—	2.63	4.2	2.90	—	4.44	—	4.32	—	—	—	1.48	0.74	1.69	0.878
$MgCl_2$	NDIS (208)	725	—	2.42	4.3	2.47	—	3.56	12 ± 1	3.62	—	3.81	5 ± 1	1.32	0.66	1.47	0.93
$MnCl_2$	ND (208)	700	—	2.50	4	2.61	—	3.58	8.4	3.62	—	—	—	1.60	0.80	1.43	—
$CaCl_2$	NDIS (213)	820	2.2	2.78	5.4	2.8	2.9	3.73	7.8	3.62	2.7	3.6	4.2	1.98	0.99	1.35	0.95
$SrCl_2$	NDIS (185)	925	2.4	2.9	6.9	2.93	2.4	3.8	9.3	3.62	3.5	4.95	13.6	2.24	1.12	1.35	—
$BaCl_2$	NDIS (214)	1025	1.4	3.1	7.7	3.16	2.5	3.86	7 ± 1	3.62	3.7	4.9	14 ± 2	2.70	1.35	1.3	—
$NiCl_2$	NDIS (215)	1022	—	2.36	4.7	2.5	—	3.8	13.8	3.62	—	4.0	6	1.38	0.69	1.61	0.99
$NiCl_2$	ND (218)	1050	—	2.28	4.4	2.5	—	3.4	—	3.62	—	—	—	1.38	0.69	1.49	—
$NiBr_2$	NDIS (215)	985	—	2.47	4.7	2.64	—	3.97	14	3.90	—	3.71	5.3	1.38	0.69	1.61	0.92
NiI_2	NDIS (215)	830	—	2.6	4.2	2.85	—	4.1	13 ± 1	4.32	—	4.6	5.3	1.38	0.69	1.57	0.88
$AlCl_3$	ND (220)	200	—	2.11	4	—	—	—	—	3.62	—	3.7	—	—	—	1.66	—
$AlBr_3$	ND (223)	140	—	2.3	4	3.3	—	3.87	7.1	3.9	—	3.1	1.8	2.7	1.35	—	1.2
$GaBr_3$	ND (223)	140	—	2.3	4	3.45	—	3.95	8.6	3.9	—	3.2	1.9	3.0	1.5	—	1.2
GaI_3	ND (223)	247	—	2.5	3.75	3.65	—	4.4	11.0	4.3	—	3.3	1.5	3.0	1.5	—	1.2
$DyCl_3$	NDIS (178)	700	—	2.65	6	3.0	—	3.5	—	3.6	—	4.2	—	2.4	1.2	1.32	1.0

[a] r_c = closest distance of approach. [b] r_s = sum of ionic radii. For details of other parameters see footnote to Table 2.

2:1 Molten halides

Following the same procedures as for 1:1 salts, NDIS experiments have been carried out on a number of 2:1 salts such as $ZnCl_2$, $MgCl_2$, $CaCl_2$, $SrCl_2$, $BaCl_2$, $NiCl_2$, $NiBr_2$ and NiI_2 (Table 3). Additionally total neutron diffraction (ND) experiments have been carried out on $ZnBr_2$, ZnI_2 and $MnCl_2$; because the coherent neutron scattering length for manganese is negative, results from ND can be used to determine accurately the nearest neighbour Mn–Cl coordination. Amongst the many important issues concerning 2:1 salts[173,183,185,206–219] is the degree of ionicity in the melt. Results for $g_{++}(r)$, $g_{--}(r)$ and $g_{+-}(r)$ show that (i) *ca.* 4 chloride ions surround each zinc ion[173] and (ii) beyond *ca.* 6 Å, $g_{++}(r)$ and $g_{--}(r)$ are phased to give complete charge cancellation, a feature characteristic of complete ionisation $ZnCl_2 \rightarrow Zn^{2+} + 2Cl^-$. The nearest-neighbour Zn–Cl distance ($r_{ZnCl} = 2.29$ Å) is found to be hardly different from any of the solid state forms, and the results show no evidence for the existence of $ZnCl^+$ or $ZnCl_3^-$ complexes of lifetime long enough to be regarded as distinct structural entities in the melt. The structure of the liquid melt is found to resemble the γ-form of the solid. The Cl^- ion structure provides tetrahedral sites for Zn^{2+}, and penetration of like ions into the first coordination shell does not occur. This situation is quite different for other 2:1 salts such as $BaCl_2$ and $SrCl_2$ (see below), where penetration effects play a major role in determining both static structure and dynamic behaviour.

Allen *et al.*[207] performed total ND measurements on molten $ZnCl_2$, $ZnBr_2$ and ZnI_2. Their results confirm a tetrahedral coordination of Zn^{2+} ions in these three molten zinc halides, and this tetrahedral structure is found to be stable to both changes in the anionic species and the temperature. Moreover, the similarity of structure in $ZnCl_2$ and $ZnBr_2$, in particular, suggests the presence of highly constrained tetrahedral units such as are usually associated with covalently bonded liquids.

Biggin *et al.*[208] employed NDIS methods to determine the three pair distribution functions for $MgCl_2$ at 725 °C. Since the solid state structure of $MnCl_2$ is similar to that of $MgCl_2$, consisting of layers made up of close-packed chloride ions with magnesium ions filling all the octahedral sites between every other layer, they also performed total neutron scattering measurements on molten $MnCl_2$. Interestingly, manganese possesses a negative scattering length, and results from a single experiment on $^{N}Mg^{N}Cl_2$ were sufficient to extract the Mn–Cl nearest-neighbour interionic separation of 2.50 Å and coordination number of 4. The results show that $MgCl_2$ and $MnCl_2$ melts are structurally similar and significantly different from that of $ZnCl_2$.

Mg^{2+} and Mn^{2+} have comparable respective radii of 0.66 and 0.80 Å, but very different electronic structures. Both ions are small compared to the chloride ion (1.81 Å), and their radii span the value for Zn^{2+} (0.74 Å). The near isomorphism between Mg^{2+} and Mn^{2+} in the liquid, together with a well defined fourfold coordination and the absence of significant penetration by small cations into the first coordination shell, confirms the hypothesis that the dominant contribution to the structure of both the solid and the liquid is the size of the cation rather than its electronic structure. However, a closer comparison between these data and those for $ZnCl_2$ reveals that the fourfold coordination of Zn^{2+} is accompanied by a true tetrahedral arrangement ($R = r_{--}/r_{+-} = 1.63$). The ionic radius of Zn^{2+} lies between Mg^{2+} and Mn^{2+}, but these melts are characterised by R-values of 1.47 and 1.43 (Table 3). Biggin *et al.*[208] concluded that the departure from tetrahedral arrangement for Mg^{2+} and Mn^{2+} is therefore not simply connected with ion size.

Biggin and Enderby[213] used the NDIS method to calculate the cation–cation, anion–anion and cation–anion pair correlation functions [$g_{++}(r)$, $g_{--}(r)$ and $g_{+-}(r)$] in $CaCl_2$ which were compared with those obtained from earlier studies on molten $BaCl_2$,[214] $SrCl_2$[183] and $ZnCl_2$.[173] The $g_{ClCl}(r)$ functions for the four systems show that, while the peak position and coordination number change little with cation size (Table 3), the peak height increases and the width decreases in moving from Ba^{2+} ($r_+ = 1.35$ Å) to Sr^{2+} (1.12 Å), to Ca^{2+} (0.99 Å) to Zn^{2+} (0.74 Å). A trend is also seen in the $g_{++}(r)$ functions with ion size; the well defined coordination exhibited by Zn^{2+} becomes less well defined and more penetration of like ions into the first coordination shell of unlike pairs occurs as the cation size increases. These results confirm the earlier view[173] that the dominant contribution to the structural properties of ionic melts with a common anion is the size of the cations and not their electronic structure.

The structure of molten $SrCl_2$ was also determined[185] by NDIS experiments. Significant differences are observed between the experimental results and simulated $g_{\alpha\beta}(r)$ based on both rigid-ion and polarisable-ion potentials.[183,185] The experimental $g_{\alpha\beta}(r)$ functions are also compared with those for $ZnCl_2$,[173] $CaCl_2$[213] and $BaCl_2$[214] by renormalising the r-scale for each salt using the sum of ionic radii ($r_+ + r_-$). The similarity of all the $SrCl_2$ and $BaCl_2$ distributions scaled by the ion sizes indicates that these two melts have similar basic structure. Since $g_{ClCl}(r)$ for molten $CaCl_2$ is found to be similar to those in the melts of $SrCl_2$ and $BaCl_2$, it is concluded that the anion structure dominates the melts with cations fitting in the interstices, as suggested by Biggin and Enderby.[213] The results show that within the molten alkaline earth chlorides $CaCl_2$, $SrCl_2$ and $BaCl_2$ the anion–anion substructure scales with cation size, while molten $ZnCl_2$ shows a clear difference extending over large distances.

The comparative absence of structure[214] in molten $BaCl_2$ beyond *ca.* 6 Å in $g_{--}(r)$ when compared with $g_{++}(r)$ is linked to the fact that the anions are mobile species. This is in accord with the fact that $BaCl_2$ becomes a fast ion conductor when it undergoes a solid-state phase transition at 1193 K, and its conductivity increases by three orders of magnitude which is also thought to be due to the high mobility of the anions in the high-temperature phase. The less mobile species are indeed found to possess more long-range order as shown by the $g_{++}(r)$ distribution where the oscillations extend to at least 10 Å. The results show that although there is a substantial amount of penetration by the anions into the first coordination shell of Ba–Cl, there is no evidence for the existence of long-lived $BaCl^+$ complexes, and rules out the ionisation scheme $MCl_2 \rightarrow MCl^+ + Cl^-$ in molten $BaCl_2$.

The three $g_{\alpha\beta}(r)$ functions relating to Ni–Ni, X–X and Ni–X correlations have been determined by NDIS in NiX_2 melts[215–217] where X = Cl, Br and I. The coordination number for anions about the cation are 4.7 ± 0.2 for $NiCl_2$,[215] 4.7 ± 0.2 for $NiBr_2$[216] and 4.2 ± 0.2 for NiI_2.[217] The smaller value in the iodide is found to be consistent with the larger amount of first-shell penetration by the nickel ions in NiI_2 relative to that in $NiCl_2$ and $NiBr_2$. The ratios r_{--}/r_{+-} in the three melts are reported in Table 3, and the results suggest an arrangement that is fairly close to being truly tetrahedral ($\sqrt{8/3} = 1.63$). Thus, nickel ions in the three melts are fourfold-coordinated and occupy tetrahedral sites in the anion structure. In comparison, nickel halides in their crystalline form possess a layered structure of $CdCl_2$-type with sixfold coordination of anions around each nickel ion. The $g_{++}(r)$ and $g_{--}(r)$ bear a close resemblance to each

other without any significant first shell penetration for both $NiCl_2$ and $NiBr_2$. In contrast, the cation–cation radial distribution of molten NiI_2 shows a broad first peak similar to the one observed previously[171,203] in molten CuCl, and the degree of overlap with the principal peak of the cation–anion distribution is so large that it leads to an extensive penetration of the nickel species into the first coordination shell. Badyal *et al.*[218] in a recent paper on molten $NiCl_2$ by ND + RMC report a value of 1.49 (Table 3) for r_{--}/r_{+-} instead of 1.61 by Newport *et al.*,[215] and suggest that its structure is best characterised as distorted octahedral (with an average of almost two vacancies leading to a coordination number close to four) rather than tetrahedral.

3:1 Molten halides

Only few 3:1 molten salts have been investigated[178,220,222,223] to date by the method of ND and NDIS. Badyal *et al.*[220] performed total ND measurements on pure molten $AlCl_3$, and analysed the results by RMC modelling. The experimental $G(r)$ results show a clear first deep minimum after the well resolved Al–Cl principal peak, thus indicating little movement of anions into and out of the first shell. A coordination number of $n_{Al}^{Cl} = 4$ along with a value of $r_{--}/r_{+-} = 1.66$ establishes a regular fourfold-coordinated tetrahedral geometry in molten $AlCl_3$. Harris *et al.*[221] from their X-ray diffraction measurements suggest a structural model for molten $AlCl_3$ as consisting of discrete Al_2Cl_6 dimers, each formed by edge-sharing of two distorted $AlCl_4^-$ tetrahedra. However, in contradiction to this model, Badyal *et al.*[220] observe predominantly chains of mainly corner-linked tetrahedral units with only partial dimerisation, and propose a 'sparse network liquid' model for molten $AlCl_3$. Since $ZnCl_2$ and $AlCl_3$ have some intriguing similarities in their physical properties such as a low melting point and very low conductivity in the melt, they suggest that the structure of molten $AlCl_3$ is similar to that of the network $ZnCl_2$ melt with the difference that in $AlCl_3$ there is much less connectivity. This seems plausible since a 3:1 salt should require less anion sharing than a 2:1 salt for achieving fourfold coordination.

Fukushima *et al.*[222] performed time-of-flight ND measurements on bismuth trihalides, BiX_3 (X = Cl, Br and I), at a number of temperatures and concluded that the pure molten BiX_3 system behaves like a molecular liquid similar to PX_3. Saboungi *et al.*[223] performed ND structural measurements on molten $AlBr_3$, $GaBr_3$ and GaI_3, and found the existence of intermediate range order (see below) in these melts. The results suggest that while there is complete dimerisation in molten $AlBr_3$ and $GaBr_3$; GaI_3 is only partly dimerised probably owing to the large size of its dimer and consequent reduced stability. Adya *et al.*[178] recently carried out a complete NDIS study of molten $DyCl_3$ and determined $g_{DyCl}(r)$, $g_{ClCl}(r)$ and $g_{DyDy}(r)$. Their preliminary analysis suggests a six-fold coordination of Cl^- ions around Dy^{3+}, and the existence of predominantly corner-sharing octahedral, $DyCl_6^{3-}$ units in the melt.

An interesting aspect of the neutron diffraction data for 2:1 and 3:1 molten salts and their mixtures is the presence of a first sharp diffraction peak (FSDP) or 'prepeak' at *ca.*1 $Å^{-1}$ in the Q-space data which is absent in the measured diffraction patterns for molten 1:1 halides. Since in the Fourier transform procedure the FSDP occurring at small values of the momentum transfer, Q, is given a relatively small weighting, the real space effect of FSDP is spread out and not well understood. The peak is felt to be a signature of intermediate range order (IRO) corresponding to interatomic correlations $\sim 2\pi/l \approx 6$ Å. For example, all three zinc halides show[207] a well resolved prepeak (at

Table 4 Structural properties of molten halide mixtures

mixed melt	*composition*	T/°C	*technique*	r_{+-}	n_{+-}	r_{--}	n_{--}	r_{--}/r_{+-}	$r_p^h/\text{Å}$
$ZnCl_2 + KCl$[a]	0% KCl	330	ND	2.28	3.93	3.71	8.6	—	1.005
		600	ND	2.29	3.67	—	—	—	0.94
	33% KCl	340	ND	2.28	4.2	—	—	—	1.00
		450	ND	2.28	3.9	—	—	—	0.98
	50% KCl	340	ND	2.26	4.1	—	—	—	1.05
		450	ND	2.28	3.8	—	—	—	1.03
	66.7% KCl	450	ND	2.28	3.9	—	—	—	1.10
	81% KCl	820	ND	2.28	4.1	—	—	—	1.12
	90% KCl	820	ND	2.31	4.7	—	—	—	—
	95% KCl	820	ND	2.29	—	—	—	—	—
	100% KCl	820	ND	3.10	6.0	4.8	12–14	1.58	—
$ZnCl_2 + KCl$[b]	60% KCl	480	NDIS	2.30	3.7	3.7	—	1.61	—
$ZnCl_2 + LiCl$[c]	0% LiCl	450	ND	—	—	—	—	—	—
	33% LiCl	450	ND	—	—	—	—	—	—
	67% LiCl	450	ND	—	—	—	—	—	—
	100% LiCl	650	ND	—	—	—	—	—	—
$NiCl_2 + KCl$[c]	0% KCl	1050	ND	2.28	4.4	—	—	1.50	—
	20% KCl	1040	ND	2.27	4.3	—	—	1.52	—
	40% KCl	1040	ND	2.26	4.2	—	—	1.58	—
	55% KCl	1040	ND	2.25	4.25	—	—	1.61	—
	70% KCl	1040	ND	2.27	4.1	—	—	1.61	—
	80% KCl	1040	ND	2.26	4.1	—	—	1.65	—
	100% KCl	1040	ND	3.10	—	4.8	—	1.58	—
$NiCl_2 + KCl$[b]	60% KCl	650	NDIS	2.28	3.6	3.6	—	1.58	—
$NiCl_2 + LiCl$[c]	0% LiCl	1050	ND	2.28	4.4	—	—	1.50	—
	33% LiCl	1040	ND	—	—	—	—	—	—
	67% LiCl	1040	ND	—	—	—	—	—	—

	100% LiCl	650	ND	—	—	—	—	—	—
$AlCl_3 + LiCl$[d]	50% LiCl	200	NDIS	2.13	3.8	3.51	4.5–6	1.65	—
$AlCl_3 + LiCl$[e]	0% LiCl	200	ND	2.11	—	3.5	—	—	0.92
	25% LiCl	280	ND	2.11	—	3.5	—	—	0.94
	50% LiCl	280	ND	2.14	—	3.5	—	—	1.18
	70% LiCl	625	ND	2.15	—	—	—	—	1.08
	100% LiCl	640	ND	—	—	—	—	—	—
$AlCl_3 + NaCl$[e]	0% NaCl	200	ND	2.11	—	3.5	—	—	0.92
	30% NaCl	300	ND	2.12	—	3.5	—	—	1.01
	45% NaCl	300	ND	2.11	—	3.5	—	—	1.10
	70% NaCl	740	ND	2.11	—	3.5	—	—	1.12
	100% NaCl	820	ND	—	—	—	—	—	—
$AlCl_3 + KCl$[f]	25% KCl	200	ND	2.2	4.5	3.5	6.8	1.59	~1
	33% KCl	200	ND	2.2	4.5	3.5	7.3	1.59	~1
$AlBr_3 + KBr$[f]	25% KBr	100	ND	2.35	4.1	3.8	8.7	1.62	~1
	33% KBr	100	ND	2.35	4.1	3.8	9.2	1.62	~1
CuCl + CuBr[g]	100% CuCl	505	ND	2.27	3.2	3.88	—	1.71	—
	75% CuCl	650	ND	2.27	2.6	—	—	—	~1.1
	50% CuCl	630	ND	2.31	2.5	—	—	—	~1.1
	25% CuCl	620	ND	2.36	2.6	—	—	—	~1.1
	10% CuCl	620	ND	2.37	2.7	—	—	—	~1.1
	0% CuCl	680	ND	2.43	3.1	3.99	—	1.64	—
AgBr + AgI[g]	100% AgBr	480	ND	2.73	4.4	3.82	—	1.40	—
	90% AgBr	540	ND	2.76	4.3	—	—	—	~1
	75% AgBr	480	ND	2.80	4.1	—	—	—	~1
	58% AgBr	530	ND	2.85	4.0	—	—	—	~1
	40% AgBr	570	ND	2.87	4.1	—	—	—	~1
	20% AgBr	630	ND	2.88	4.2	—	—	—	~1
	0% AgBr	660	ND	2.90	4.5	4.44	—	1.53	—

[a]Ref. 174. [b]Ref. 226. [c]Ref. 218. [d]Ref. 227. [e]Ref. 220. [f]Ref. 228. [g]Ref. 229. r_p^h = positions of prepeak, see footnote to Table 2 for details of other parameters. In the mixtures with a common anion the + sign in r_{+-} and n_{+-} refers to the cation other than the alkali-metal ion. In mixtures with a common cation the − sign in r_{+-} and n_{+-} does not distinguish between the two types of anions.

ca. 1 $Å^{-1}$) in the total structure factors $S(Q)$ and, a significant shift in the position of the prepeak to a lower Q-value, both with increased temperature and increased anionic size is observed. Moreover, the height of this prepeak increases with increasing anion size or decreasing ionicity, from chloride to bromide to iodide. This trend reflects the highest degree of intermediate range order (IRO) in the iodide where the short-range ordering appears to be the weakest. As another example, the existence of prepeaks[215,216] in molten $NiCl_2$, $NiBr_2$ and NiI_2 at $Q = 0.99$, 0.92 and 0.88 $Å^{-1}$, respectively, which bear a close resemblance to the respective Bragg peaks at $Q = 1.09$, 1.03 and 0.96 $Å^{-1}$, suggests that the layered structure between planes of Ni^{2+} ions seen in the solid, is retained in the melt.

Amongst the many theoretical and computer simulation attempts to identify the origin of this FSDP, principally in 2:1 systems, the most successful have been those of Salmon[224,225] and Wilson and Madden.[191] The latter used a simple polarisable ion model (PIM) without involving the concept of charge transfer, and computer simulations based on this model, unlike those based on the rigid ion model (RIM),[182,187] are found to reproduce qualitatively the observed experimental features such as the overlap of principal peaks in $g_{++}(r)$ and $g_{--}(r)$ as well as the FSDP in $S_{++}(Q)$. However, it is to be stressed that for quantitative agreement between experimental and calculated $g(r)$ functions, more refined potentials are needed for 2:1 and 3:1 systems.

Molten halide mixtures

Molten salt mixtures often exhibit rich phase behaviour and attractive properties such as low-temperature eutectics which are of value in commercial applications such as energy storage systems. Their thermodynamic and physical properties display strong compositional dependence. However, until recently there has been a comparative lack of structural information on such mixtures which is due, in part, to their increased complexity. While the structure of a pure molten salt containing two distinct species can be described in terms of three partial radial distribution functions $g_{\alpha\beta}(r)$, a binary mixture of three distinct species (*e.g.* XCl_n/YCl_n) has six $g_{\alpha\beta}(r)$ functions.

Neutron diffraction studies continue to provide information on a growing number of metal halide/alkali halide mixtures.[174,218,220,226–229] Structural investigations have mainly been carried out at the total diffraction level, although three studies have been made with isotopes (Table 4). Interpretation of structural information from total patterns are usually assisted by monitoring how $G(r)$ changes with concentration of one component. Additionally, advanced modelling techniques such as reverse Monte Carlo (RMC) methods are used to estimate the degree and extent of particular structural units in the molten mixtures.[220,226,228]

Neutron diffraction results show that $NiCl_2$–LiCl and $ZnCl_2$–LiCl mixtures exhibit simple admixture structural behaviour.[218] The Li^+ ions (being similar in size to Ni^{2+} or Zn^{2+}), compete equally well with Ni^{2+} or Zn^{2+} cations for Cl^- ions so that the local structure around each type of cation remains practically the same as in the pure component salts. In contrast, a considerable structural modification is observed in the $NiCl_2$–KCl molten system[218] with larger alkali cation, K^+. The large and weakly polarising K^+ ion is unable to compete effectively with the Ni^{2+} for the anions, and strengthens the local structure of the Ni^{2+} ion at its own expense. The values of r_{--}/r_{+-} and coordination number (Table 4) suggest that the local geometry of the Ni^{2+} ion changes from a distorted octahedron with vacancies to almost regular

tetrahedral with increasing KCl concentrations. In $ZnCl_2$/KCl and $NiCl_2$/KCl, the existence of a prepeak or FSDP in the scattering data is indicative of IRO brought about by strong correlations due to the divalent cations, and ordering between tetrahedral MCl_4^{2-} units.

Similarly, diffraction patterns of $AlCl_3$/LiCl and $AlCl_3$/NaCl also exhibit[220] a FSDP in the diffraction data which as mentioned above is indicative of IRO. Biggin *et al.*[227] performed NDIS measurements on a $(AlCl_3)_{0.5}(LiCl)_{0.5}$ melt and derived $g_{AlCl}(r)$, $g_{AlAl}(r)$ and $g_{ClCl}(r)$. The results indicate a tetrahedral distribution of Cl^- ions around Al^{3+}, and confirm the existence of well defined $AlCl_4^-$ tetrahedra in the melt. The structureless form of $g_{AlAl}(r)$ suggests very little Al–Cl–Al bridging between these tetrahedra. Badyal *et al.*[220] performed total ND experiments on $AlCl_3$ + LiCl and $AlCl_3$ + NaCl mixtures covering the entire composition range. The results suggest that the connectivity in the structure of pure molten $AlCl_3$ through chains of corner-linked tetrahedral units formed by Al–Cl–Al bridges, is proportionately reduced upon the addition of alkali halide. The RMC modelling results[220] for $(AlCl_3)_{0.5}(LiCl)_{0.5}$ with smaller Li^+ ion suggest that two neighbouring $AlCl_4^-$ tetrahedra approach the central Li^+ ion resulting in an approximately octahedral cage for the alkali cation. However, results for $(AlCl_3)_{0.5}(NaCl)_{0.5}$ are found to be consistent with the Na^+ ion occupying disordered sites in the face centres of tetrahedra. These results also suggest a lower average distance between neighbouring tetrahedra in the case of Li^+ leading to an IRO on a shorter length scale as compared to that in the case of Na^+ (Table 4).

The structure of molten salt mixtures $(AlX_3)_{0.67}(KX)_{0.33}$ and $(AlX_3)_{0.75}(KX)_{0.25}$, both for X = Cl and Br, has also been investigated by ND.[228] All four structure factors exhibit a FSDP at *ca.* 1 $Å^{-1}$. Though the ND results (Table 4) imply a tetrahedral coordination of X atoms about each Al, this does not preclude the existence of other structural units and, in fact, model calculations based on random packing of structural units reveal[228] the presence of $Al_2X_7^-$ and $Al_3X_{10}^-$ anionic species in the mixed melts.

Shirakawa *et al.*[229] carried out ND experiments on non-ideal mixed molten salts $(CuCl)_x$–$(CuBr)_{1-x}$ and $(AgBr)_x$–$(AgI)_{1-x}$ along their liquidus curves. The non-ideality of these mixtures is manifested by the concentration dependence of the nearest-neighbour interionic distances (r_{+-}). Moreover, r_{+-} deviates appreciably from that obtained by linear interpolation of the equivalent result in the pure molten salts.[203,205,230,231] Interestingly, as x is increased r_{+-} in CuCl–CuBr shows a relative contraction while in AgBr–AgI it shows a relative expansion.

Molten nitrates

Molten nitrates have relatively low melting points and provide low-temperature baths which are important to industry. They show superior glass-forming tendencies owing to the tendency of the nitrate ion to resist reorientation in the disordered phase. They have been found to be essential ingredients in many industrial explosives and fertilisers, and exhibit rich phase behaviour on mixing with other nitrates or when dissolved at high concentrations in water.

In the first comprehensive structural study of molten $LiNO_3$, Adya *et al.*[176] and Kameda *et al.*[232] used NDIS to determine the ion–ion and the ion–counterion pair rdf's. Kameda *et al.* reported the five partials $g_{LiN}(r)$, $g_{LiO}(r)$, $g_{NN}(r)$, $g_{NO}(r)$ and $g_{OO}(r)$ from their ND measurements on a neutron spallation source. Adya *et al.* reported the

pair rdf's $g_{LiLi}(r)$, $g_{LiN}(r)$ and $g_{LiO}(r)$ from their ND data gathered at instruments at a reactor. Their results provided new information on the Li^+–Li^+ coordination, and a useful comparison between the results obtained at the rdf level on two different neutron sources. Agreement between the structural information derived from experiments on two different sources is found to be excellent insofar as the nearest-neighbour coordination as defined by $g_{LiN}(r)$ and $g_{LiO}(r)$ is concerned. However, discrepancies appear between the two results in the range of second coordination shell and beyond. In particular, the two studies reveal that the lithium monovalent cation is surrounded on an average by four nitrate (NO_3^-) ions; one oxygen atom in each of these NO_3^- ions facing towards Li^+. The space and time-averaged local structure of $LiNO_3$ in the molten state is found to be appreciably different from that in its crystalline state.[232] The results for $g_{LiLi}(r)$ [or $g_{++}(r)$] with $r_{LiLi} = 4.1$ Å are found to be significantly different from $g_{NN}(r)$ [or $g_{--}(r)$] with $r_{NN} = 4.8$ Å, thus raising question regarding the general applicability of primitive modelling of monovalent molten salts.The nearest-neighbour Li–O and Li–Li distances of 1.86 and 3.86 Å reported in an earlier MD study[189] are found to be significantly less than the values of 2.1 and 4.1 Å reported from the use of NDIS technique, thus reflecting uncertainties in the effective pair potentials employed in the MD study.

Neutron diffraction studies of metal nitrate systems[189,234,235] were initially used to confirm X-ray results[236,237] which show that nitrate ions coordinated to six nearest-neighbour cations in molten $LiNO_3$ and $AgNO_3$, but to only three cations in other molten alkali nitrates. From this work, it is proposed that nitrate ions and their counter cations form a diamond-like arrangement with random vacancies in molten $NaNO_3$, KNO_3, $RbNO_3$ and $CsNO_3$, and a simple cubic structure for molten $LiNO_3$ and $AgNO_3$. These suggested structures have been called into question when ND experiments were carried out on molten MNO_3 (M = Li, Na, K, Rb, Cs, Ag and Tl).

Results of neutron diffraction studies on molten monovalent metal nitrates, MNO_3 (M = Li, Na, K, Rb, Cs, Ag and Tl) by the time-of-flight technique on a pulsed neutron source confirm[234] the above observations of a distorted C_{2v} symmetry of the NO_3^- ion in molten $LiNO_3$, $AgNO_3$ and $TlNO_3$ due to specific cation–anion interactions, and a D_{3h} symmetry for the NO_3^- ion in molten $NaNO_3$, KNO_3, $RbNO_3$ and $CsNO_3$. However, Yamaguchi *et al.*[235] carried out a subsequent pulsed ND study of molten $LiNO_3$, $RbNO_3$ and $AgNO_3$, and analysed their data by applying a least-squares analysis to the intra-ionic part of the total structure factors. Their results reveal the geometry of the nitrate ions to be equilateral triangular with D_{3h} symmetry in $LiNO_3$, $AgNO_3$ and $RbNO_3$ melts, independent of the cation involved, in contradiction to the earlier observations of Suzuki and Fukushima.[234]

A detailed NDIS study[175] has also been undertaken on the interatomic structure of deuteriated molten ammonium nitrate, $N(1)D_4N(2)O_3$. The results show the existence of stable ND_2^+ and NO_3^- ions in the melt; the ND_4^+ ions conform to the tetrahedral geometry and the NO_3^- ions retain their D_{3h} symmetry arising from an equilateral triangular geometry. With a weak cation such as ND_4^+, no extensive rearrangement is found to occur during the fusion process for molten ammonium nitrate; NO_3^- ions are not affected by the weak cationic environment. The results for the 'cross' pair distribution function $g_{N(1)N(2)}(r)$ suggest that the crystal structure[233] relaxes significantly on melting, especially with regard to the nearest-neighbour cation–anion interactions.

Mixtures of molten nitrates

Two ND studies have so far been made on molten nitrate mixtures. With the use of model fits to the experimental data for 1:1 $LiNO_3$–$RbNO_3$, the results[235] show that the Li–O coordination number is in the range 3–4 at 1.9 Å in agreement with that found in pure molten $LiNO_3$. An NDIS study of $ND_4NO_3/Ca(NO_3)_2$ at its eutectic concentration, shows[177] that the local coordinations of ND_4^+ and NO_3^- are similar to those in pure molten ammonium nitrate. However, the results for the 'cross' term reveal that the $N(1)D_4^+ \cdots N(2)O_3^-$ coordination is significantly different from that in pure molten $N(1)D_4N(2)O_3$.[175] Moreover, there is an overall relaxation of the structure on the addition of $Ca(NO_3)_2$. This effect is also observed[238] when D_2O is mixed with ND_4NO_3 at a 1:1 molecular ratio.

Miscellaneous melts

Andonov *et al.*[239] investigated the structure of molten lithium metaniobate, $LiNbO_3$ over a range of temperature, and found that (i) octahedral NbO_6 molecules present in its crystalline form persist up to 100 K above its melting point, and (ii) the melt consists of corner-sharing NbO_6 octahedra bonded together by Li atoms.

Amongst the many outstanding challenges two are particularly relevant: (i) determination of real interatomic potentials for 2:1 and 3:1 molten systems which mimic the experimental $g(r)$ and (ii) and characterisation of the structure in molten salt mixtures.

Water

Water and heavy water (D_2O) in particular have been the most frequently studied of all liquids by neutron diffraction methods. In recent years, the application of NDIS methods to water/heavy water mixtures has facilitated the determination of all three radial distribution functions, $g_{HH}(r)$, $g_{OH}(r)$ and $g_{OO}(r)$[240] (Fig. 4), which have been used to identify the structural aspects of hydrogen bonding and to check the reliability of computer simulation studies on potential models for water.[241]

Because of the importance of water as a universal solvent, many neutron diffraction studies have also been carried out under non-ambient conditions. The structural investigations of Texeira, Bellissent-Funel and co-workers on supercooled and amorphous heavy water often under pressure, gives insight into the origins of its anomalous behaviour at low temperatures.[242,243] At the other extreme, Soper, Ricci and colleagues have investigated water structure up to and beyond its critical point.[244–247] By focussing on the hydrogen bonding as defined by $g_{OH}(r)$ and $g_{HH}(r)$, they have been able to quantify structural changes which are accompanied by changes in temperature and density. In particular, they have shown that the hydrogen bonding as defined by the relatively small peak ≈ 2 Å in $g_{OH}(r)$ is considerably affected by extremes of temperature; more so than would be inferred from simple energetic calculations based on a comparison of k_BT with the hydrogen bond energy.[247] Moreover, the results are appreciably different from those of simulation based on the use of pair potential models for water.[248–250] The challenge here is twofold: (i) to gather more accurate information in order to help comprehend the large amount of thermodynamic and spectroscopic information, and (ii) to use this information to examine the accuracy of model pair potentials, and suggest how they must be modified to match the experimental results.

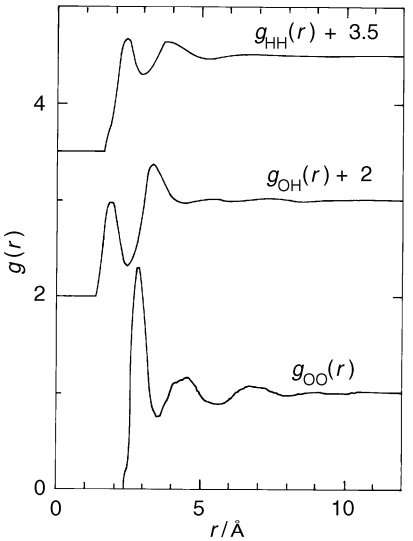

Fig. 4 The three radial pair distribution functions for water at ambient conditions.[241]

Aqueous solutions

Electrolytes in water

Neutron diffraction studies on aqueous electrolyte solutions of the form of a salt (MX_n) in water (H_2O) or heavy water (D_2O), have been carried out since the late 1960s.[251] In the early 1970s Enderby, Neilson and co-workers[252] applied the method of isotopic substitution to aqueous solutions of nickel chloride and sodium chloride in heavy water, and demonstrated that quantitative information could be obtained on the ionic hydration structure of both Ni^{2+} and Cl^- ions.[253] Total ion specific radial distribution functions are of the form given in eqn. (1), which for concentrations $\sim 1\,mol\,kg^{-1}$ can be approximated to

$$G_I(r) \cong Ag_{IO}(r) + Bg_{ID}(r) + E$$

Analysis of this function gives the hydration number $\bar{n}_I$ and aqua ion conformation.[253] First shell coordination numbers $\bar{n}_I$ can be calculated in three different ways. For cations, where the I···O peak is well resolved, integration of $G_I(r)$ over the range defined by the correlation in $g_{IO}(r)$ according to eqn. (2) gives the appropriate hydration number. For anions, where the nearest neighbour I···H(D) peak is well resolved, integration of $G_I(r)$ over the range of the correlation $g_{ID}(r)$ according to eqn. (2) gives the anion hydration number. Where individual peaks are not well resolved, as in the case of K^+, integration of $G_I(r)$ over the entire range and the condition $n_I^D \equiv 2n_I^O$ will give the total number of water molecules in the hydration shell. There already exists an extensive literature on the hydration properties of ions, and results are available for many cations and a few anions (Table 5).

Since our previous review of the subject in 1990,[254] several new developments have

occurred. Most notable has been the use of NDIS data from an aqueous nickel chloride solution containing H_2O–D_2O mixtures to determine $g_{ClH}(r)$ and $g_{ClO}(r)$ independently[255] (Fig. 5). As a result it is now possible to assess the accuracy of computer simulation calculations of $Cl\cdots H_2O$ model potentials.[255–257] Additionally, a detailed study of Li^+ hydration as a function of concentration in lithium chloride solutions in heavy water has confirmed the hydration number is *ca.* 6 at concentrations below 4 mol kg^{-1}.[258] It is likely that this value will be the limiting value for $\bar{n}_{Li}^{D_2O}$. The results of this study were also compared with *ab initio* molecular orbital calculations of $[Li\cdots(H_2O)_n]$ configurations;[259] good agreement is found between experiment and simulation for r_{LiO}, but the r_{LiH} distance is calculated to be significantly larger, at 2.6 Å, than found experimentally (Table 5). The discrepancy is probably due to a dominance of the ion–dipole interaction and the neglect of effects due to dipole–dipole interactions of the water molecules.

By following the same NDIS methodology applied to nitrogen atoms (^{14}N,^{15}N), the Japanese group of Kameda has been gathering information on the aqua structures of the anions NO_3^-, NO_2^- and SCN^-.[276–278] The results suggest that each of these has its own characteristic local structure with well defined short-range nearest-neighbour correlations to H(D) atoms (Table 5).

Because of a growing technological interest in the properties of aqueous electrolyte fluids in the supercritical region, most notably in their breakdown of toxic waste materials,[279] NDIS experiments have been undertaken at temperatures and pressures up to and beyond their critical points. Investigation of the hydration structures of Li^+, Ni^{2+} and Cl^- shows all three aquasions to be highly susceptible to changes in temperature.[280–284] Generally there is a reduction in hydration number (Table 6), presumably accompanied by an increase in anion–cation contacts. For the case of Ni^{2+} there is also an interesting effect caused by the anions: the hydration sphere of Ni^{2+} is more completely destroyed in aqueous nickel sulfate than in aqueous nickel chloride at the same temperature.

A similar progressive depletion of the Cl^- hydration sphere is observed in aqueous chloride solutions, and is taken as evidence for a commensurate growth in anion–cation contacts.[281,283,284]

With the commissioning of the SANDALS diffractometer on ISIS at Rutherford Appleton Laboratory, it has become possible to use H_2O–D_2O mixtures in the determination of solvent structure in solutions. A study of two lithium chloride solutions[285] shows that whereas the water structure at 1 mol kg^{-1} is closely similar to that of pure water, at an ionic concentration of 10 mol kg^{-1}, there is considerable disruption of the water network with a reduction by 70% of the number of hydrogen bonds. This result stands in marked contrast to that for a 10 mol kg^{-1} urea water solution, where the water structure remains unperturbed by the large amount of apolar solute.[286]

Recent work at elevated temperature on 1 mol kg^{-1} sodium chloride[287] indicates that the water structure changes significantly with temperature and is akin to the change observed in pure water,[246,247] with a progressive shift to larger distances of the $O\cdots H$ hydrogen bond correlation at *ca.* 2 Å, and its eventual disappearance at 450 °C.

In an attempt to quantify the effect of anions on water solvent structure, Leberman and Soper[288] carried out NDIS experiments on three equimolal solutions of ammonium nitrate, sodium nitrate and sodium chloride in water–heavy water mixtures.

Table 5 Aqua ion coordination derived from neutron diffraction isotopic substitution methods. Where possible the lowest concentration is given

ion	*solute* (*molality*)	$r_{IO}/\AA$	$r_{ID}/\AA$	$\bar{n}_I$	*ref.*	*comments*[a]
Li^+	LiCl (3.6)	1.95(2)	2.52(2)	6.0(5)	258	n_1 depends on counterion and concentration
	LiCl (1)	1.96(2)	2.52(2)	6.5(10)	258	
ND_4^+	ND_4Cl (5)	2.8–3.2	3.4–3.8	10–12	260	
K^+	KCl (4)	2.9–3.4		5.3(6)	261	unresolved first shell
Ca^{2+}	$CaCl_2$ (1)	2.46(3)	3.07(3)	10.0(6)	262	n_1 depends on concentration
	$CaCl_2$ (4.5)	2.41(3)	3.04(3)	6.4(3)	262	
Cr^{3+}	$Cr(ClO_4)_3$ (2.22)	1.98(2)	2.60(3)	6.0(5)	263	
Fe^{2+}	$FeCl_2$ (1.06 + 1.2 HCl)	2.12(2)	2.75(5)	6.0(3)	264	
Fe^{3+}	$Fe(NO_3)_3$ (1.6 + 1.6 DNO_3)	2.01(2)	2.68(3)	6.0(3)	265	
	$Fe(ClO_4)_3$ (2.48 + 1.0 $DClO_4$)	2.01(2)	2.65(3)	6.3(3)	265	
Ni^{2+}	$NiCl_2$ (1.46)	2.07(2)	2.67(2)	5.8(2)	266	
	$Ni(ClO_4)_2$ (3.8)	2.07(2)	2.67(2)	5.8(2)	267	
Cu^{2+}	$CuCl_2$ (4)	1.96(3)	2.58(3)	3.3(2)	268	C. hydration depends on counterion and concentration
	$Cu(ClO_4)_2$ (2)	1.96(3)	2.58(3)	4.1(2)	268	
	$Cu(NO_3)_2$ (1)	1.96(3)	—	4.6(2)	269	
Zn^{2+}	$Zn(CF_3SO_3)_2$ (2)	2.09(2)	2.69(2)	5.3(2)	270	
	$ZnCl_2$ (4)	2.09(2)	2.74(4)	4.1	270	C. $\sim$ 1.4 Cl^- at 2.28 Å in first coordination shell
Ag^+	$AgClO_4$ (4.16 + 0.59 $DClO_4$)	2.41(2)	2.97(4)	4.1(3)	271	

Nd^{3+}	$NdCl_3$ (2.85)	2.48(1)	3.13(2)	8.5(2)	272
Dy^{3+}	$DyCl_3$ (0.97 + 0.1 DCl)	2.39(2)	3.03(2)	7.9(2)	273
	$Dy(ClO_4)_3$ (0.3 + 0.12 $DClO_4$)	2.40(2)	3.03(2)	8.0(2)	274
Yb^{3+}	$Yb(ClO_4)_3$ (1.0 + 0.12 $DClO_4$)	2.32(2)	2.59(2)	9.2(2)	274
Cl^-	$NiCl_2$ (2)	3.1(1)	2.28(3)	6.4(3)	255
ClO_4^-	$NaClO_4$	3.7	~2.9	4.5(5)	275
NO_2^-	$NaNO_2$ (10 mol % = 5.6)	~3.5	2.71(2)	3.7(5)	276
NO_3^-	$NaNO_3$ (10 mol % = 5.6)	~3.8	2.80	5.0(5)	277
SCN^-	NaSCN (10 mol % = 5.6)	—	2.16	1.8(2)	278

[a]The letter C indicates cation–anion contacts.

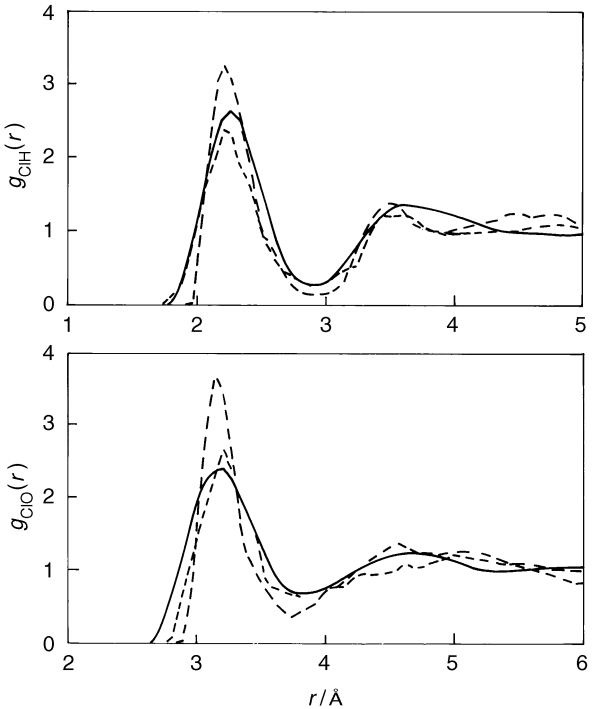

Fig. 5 The radial distribution functions $g_{ClH}(r)$ and $g_{ClO}(r)$ (full curve) obtained from neutron diffraction experiments,[255] on an aqueous solution of $2\,mol\,kg^{-1}$ nickel chloride, compared with simulation results of Sprik *et al.*[256] (short dashed curves) and Dang *et al.*[257] (long dashed curves).

Calculations based on changes in the pair distribution function $g_{HH}(r)$ between pairs of solutions allowed them to establish a correlation between the 'induced pressure of a particular anionic species with its efficacy in precipitating or salting-out protein from solution'. This information is aimed at helping explain the basic origins of the Hofmeister series of anions which have progressively larger effects on salting out of proteins.[289]

Results on solute structure are continuing to become available for a few select systems at relatively high concentrations. Within the past few years second difference experiments have been carried out on heavy water solutions of lithium chloride,[290] copper chloride,[291] nickel nitrate and nickel sulfate.[292]

The main focus of the lithium chloride study was to monitor changes in $g_{ClCl}(r)$ with concentration and examine in detail the results of theoretical model calculations which suggest direct $Cl^- \cdots Cl^-$ contacts exist, even at infinite dilution.[295] The experimental results at $8.6\,mol\,kg^{-1}$ in LiCl show that although there are still direct contacts between chloride ions, the coordination number is about 30% of that at $14\,mol\,kg^{-1}$, and suggests that such contacts will become negligible at concentrations below *ca.*

Table 6 Hydration properties of ions in aqueous solutions at elevated pressures and temperatures, with errors in parentheses

ion	*solute*	*molality* *mol kg*$^{-1}$	*pressure/* *bar*	*temperature/* °*C*	r_{IO}	r_{ID}	$\bar{n}_I$	*ref.*
Ni^{2+}	$NiCl_2$	2	1	25	2.06(2)	2.67(2)	5.9(2)	266
	$NiCl_2$	3	300	90	2.08(5)	2.68(3)	6.3(5)	280
	$NiCl_2$	3	1500	150	2.04(5)	2.64(3)	5.3(4)	280
	$NiCl_2$	2	1000	100	2.05(3)	2.67(5)	5.7(5)	281
	$NiCl_2$	2	1000	300	~2.1	~2.5	4.5(5)	281
	$NiSO_4$	1.2	1000	300	—	—	—	282
Cl^-	$NiCl_2$	2	1	25	3.1(1)	2.28(3)	6.4(3)	255
	$NiCl_2$	2	1000	100	3.3(2)	2.30(3)	6.9(5)	281
	$NiCl_2$	2	1000	300	3.4(2)	2.39(4)	4.9(5)	„
	LiCl	[a]	1690	375	—	2.33(2)	2.5(2)	283
	LiCl	3.02	1690	197	—	2.31(1)	4.5(1)	284

[a] mol dm^{-3}.

1 mol kg^{-1}. By contrast, in nickel chloride at the same chloride concentration there is no evidence of direct contacts between chloride ions.[293]

The study of copper chloride was aimed at resolving the structure of the nearest neighbour Cu^{2+} coordination shell, which contains both Cl^- and water molecules.[291] The results show that direct contacts exist between Cu^{2+} and Cl^- with a coordination number $\bar{n}_{Cu} = 2.5(5)$ in the range $2.6 \leq r/\text{Å} \leq 4.4$. Additionally, analysis of $g_{ClCl}(r)$ shows direct contacts between Cl^- ions, with a value of $\bar{n}_{Cl}^{Cl} = 3(0.5)$ and is consistent with a six-fold coordination of Cl^-. The NDIS studies of the nickel sulfate and nickel nitrate solutions were carried out to investigate the dependence of $g_{NiNi}(r)$ on counter-ion.[292] Skipper and Neilson identified an appreciable change in this function on exchange of anion from Cl^- to Br^-.[294]

Although there is now a large body of knowledge on the structure of aqueous electrolytes there remains much to be undertaken, which will help interpret neutron diffraction data obtained for more complex systems such as aqueous solutions of polyelectrolytes and biopolymers. Moreover, at the level of second differences, a knowledge of ion–ion pair distribution functions will be useful in assessing the validity of primitive model (PM) calculations in ionic solutions.[295,296]

Polyelectrolytes in water

Extension of the NDIS methods to liquids containing large molecules is straightforward, although the analysis necessarily becomes more complicated. However, by focussing on particular aspects of the structure, *e.g.* the aqueous solvent, the ionic hydration or the coordination of water molecules to a specific part of the solute molecule, useful structural information can be derived from the experimental data.

The first studies on polyelectrolytes (PE) were undertaken by van der Maarel *et al.*,[297] who investigated the hydration of Li^+ in polyacrylate solutions. Results show that the Li^+ hydration is relatively unaffected by the presence of the polyacrylic acid (PAA). By contrast, a recent study by Tromp and Neilson[298] showed that in cross-linked polysty-

Table 7 Hydration of ions in aqueous polyelectrolyte solutions

ion	*polyelectrolyte* (*monomer molality*)	$r_{IO}/Å$	$r_{ID}/Å$	$\bar{n}_I^O$	$\bar{n}_I^D$	*ref.*
Li^+	polyacrylate (–[$CH_2CHCOOH$]) (1.21)	1.97(2)	2.51(2)	4.5(5)	9(1)	296
	[$^2H_2$]polyacrylate ([$CD_2CHCOOH$]) (1.21)	1.97(2)	2.51(2)	4.5(5)	9(1)	296
	cross-linked polystyrene sulfonate exchange resin (4.6)	1.95(2)	2.4(1)	5(1)	7.5(2.0)	298
Ni^{2+}	polystyrene sulfonate (2)	2.05(2)	2.63(3)	6(1)	9(2)	299
	cross-linked polystyrene sulfonate exchange resin (2)	2.06(2)	2.70(2)	6(1)	9(2)	299
Cl^-	linear poly(ethyleneimine) (–[$CH_2CH_2ND]_n^-$) (1.5)	—	2.30(5)	6.5(4)	—	300

rene sulfonate (PSS) solution the Li^+ hydration is seriously disrupted by the presence of the polyion (Fig. 6). Also in cross-linked PSS solution the Ni^{2+} coordination, as defined through $G_{Ni}(r)$, has a similar shape to that found in ordinary electrolyte solutions such as $NiCl_2$ in water.[299] However, there is clear evidence that the Ni^{2+} is strongly coordinated to the polyion. This is demonstrated by the fact that the coordination number associated with the $Ni^{2+} \cdots D$ correlations is appreciably less than twice that for the $Ni^{2+} \cdots O$ correlations (Table 7). The difference between the behaviour of Li^+ and Ni^{2+} in cross–linked PSS solution is believed to be due to the weaker hydration of Li^+ whose hydration shell is relatively easily disrupted compared to that of Ni^{2+}, and whose water molecules are more susceptible to the polarisation effects of the sulfonate groups on the PSS. As a result the D_2O molecules of the Li^+ hydration shell are more closely packed than in ordinary electrolyte solution.[258] A similar study of a 1.8 mol kg^{-1} Ni^{2+} non-cross-linked PSS heavy water solution showed that the Ni^{2+} coordination is the same as that in a solution containing the cross-linked polymer, and clearly suggests a direct link between the Ni^{2+} and the SO_3^- group of PSS.

The behaviour of anions is also of interest in PE solutions, and a study by Bieze *et al.* showed that the presence of a linear polyion such as a polyethylene imine seriously affects the first hydration shell of Cl^-, and suggests close contacts can exist between the polyelectrolyte and the counterion.[300] This observation is consistent with results of Cl^- nuclear magnetic relaxation rates which are strongly enhanced by the presence of the polycation.

From a slightly different point of view, Bieze and co-workers[301] investigated the hydration properties of the non-ionic surfactant polyethylene oxide (PEO). They applied the first difference NDIS method to 1.88 monomolal aqueous deuteriated and hydrogenated PEO, and calculated the total distribution function $G_{Hp}(r)$ of the polymer protons. This function showed no evidence of structured water in the neighbourhood of the polymer. Furthermore the results show that an average of six water molecules can be packed around the surface of the monomeric unit.

It is clear that much remains to be done on these systems, and plans are already in hand to use the biological polyelectrolyte DNA as a system on which many other

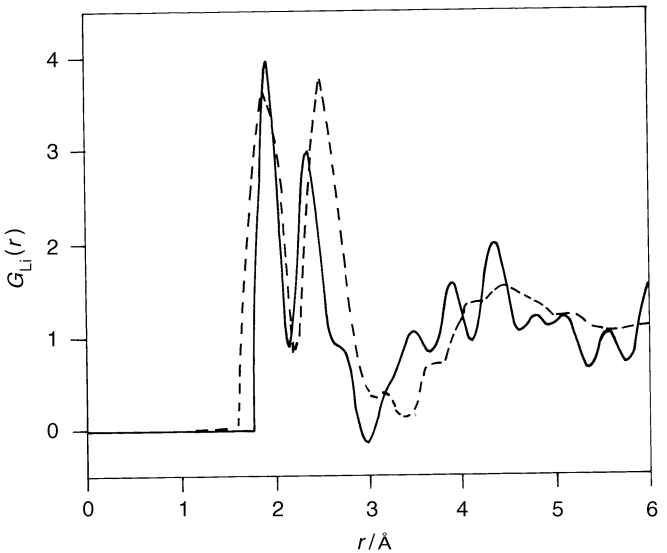

Fig. 6 The total lithium ion pair distribution function $G_{Li}(r)$ obtained in a 4.6 mol kg^{-1} lithium polystyrene sulfonate exchange resin in heavy water (full curve) and in 3.6 mol kg^{-1} lithium chloride in heavy water (dashed curve).[258] The data have been normalised to correspond to the same concentration in both cases.

NDIS experiments can be carried out.[302] The advantage of this system is that many more controls can be made of the basic polymeric unit, and studies can more readily be made of structure as a function of polymer length and shape, counterion (both positive and negative) concentration, pH, *etc.*

Biomolecular aqueous solutions

Shortly after the introduction of NDIS methods to the study of structure in aqueous electrolytes, Finney and Turner initiated investigations of biologically significant molecules in water.[303] Beginning with urea $OC(ND_2)_2$[286,304,305] they demonstrated how NDIS applied to the nitrogen atoms could be used to determine the local hydration structure around ND_2 groups, and provide confirmation of computer simulation studies of aqueous urea solutions.[306] Since then, they have widened their investigations to include systems such as tetramethylammonium chloride (TMACl) in water,[307,308] and methanol–water mixtures.[309] In collaboration with Soper they showed how the custom-built SANDALS diffractometer at ISIS (Rutherford Appleton Laboratory) could be used to obtain information on all three aspects of the TMACl–water system, *i.e.* the solute, the solvent and the solute–solvent structure. As a result, a comprehensive picture is beginning to emerge of the structure in TMACl solutions: (i) the Cl^- hydration is similar to that in many other aqueous electrolyte solutions; (ii) the TMA is predominantly apolar in character; (iii) the water structure is not significantly different from that found in pure water, even when the solute concen-

tration is such that there is only one layer of water molecules around each ion; (iv) the correlation between TMA centres is situated at *ca.* 4.7 Å. The results of a similar study of a 1.9 mol dm^{-3} methanol–water mixture confirms the existence of a hydration shell of water molecules at a distance of *ca.* 3.7 Å from the carbon atom of the CH_3OH molecule. The water molecules in this shell form a disordered cage but retain the roughly tetrahedral local coordination found in pure water.

In an attempt to understand the competing effects of hydrophillic and hydrophobic groups in aqueous solution, Soper and Luzar have applied similar techniques to investigate the conformation of water around the biological co-solvent dimethyl sulfoxide.[310] NDIS methods were applied to the water molecules in a concentrated solution of $(DMSO)_1{\cdot}(H_2O)_2$, and used to obtain $g_{HH}(r)$. They also used isotopic substitution on the methyl protons, M, and determined $g_{MM}(r)$ and the cross-term $g_{MH}(r)$. The results show 'the pronounced contrast in structure of the water of hydration around DMSO, with the oxygen atom strongly hydrogen bonded, but the methyl groups surrounded by a loose hydrogen-bonded cage of water molecules'. Perhaps not surprisingly at such high solute concentrations the water structure itself is more pronounced than in pure water, a consequence of the 'strong hydrogen bonding of water to the DMSO oxygen atom'.

In recent years the same methods of NDIS plus spherical harmonic analysis have been extended to more complex aqueous solutions. Studies of the hydration of acetylcholine $[H_3C–C{=}O–O–CH_2–CH_2N^+(CH_3)_3]$ show that water molecules form a disordered cage around the head group with very little disruption to the general water structure in solution.[311] Moreover, an investigation of both the local and long-range structure of water in the perfluorinated nickel substituted amorphous Nafion membrane has been made by a combination of small angle neutron scattering (SANS) and NDIS techniques. Pair distribution functions of the various species in the solution have been measured on a scale from 1 to 100 Å. Amongst other things, it is found that the water structure is similar to that in bulk water, which is consistent with the continuous random network model.

Using a slightly different approach, Gullidge and Neilson applied the first difference method to Ni^{2+} in an aqueous solution of 0.5 mol kg^{-1} adenosine triphosphate (ATP).[312] The results showed clearly that the Ni^{2+} cation is directly bonded to the phosphate moiety of the ATP, and substantiates information inferred from NMR studies.[313] Work at this level has recently been extended to the structure around ions in aqueous solutions containing biopolymers such as DNA and RNA. In the first of a series of investigations, Wilson *et al.* have shown how Cl^- hydration is modified by the presence of large molecules such as glycine and poly-glycine.[302]

Besides the role of the counterions in such solutions, it is also necessary to discover the structural aspects of all parts of the solution. For example, it will be particularly interesting to determine how the conformation of biomolecules such as proteins depends on counterions, especially those anions in the Hofmeister series.[288,289]

Apolar molecules in water

The NDIS method can be used to probe the fundamental aspects of the hydrophobicity, the generic term used to describe such contrasting behaviour as the immiscibility of oil and water and the manner in which proteins fold in an aqueous environment. Small apolar species, such as argon, krypton, xenon, methane (CH_4), *etc.* are sparingly

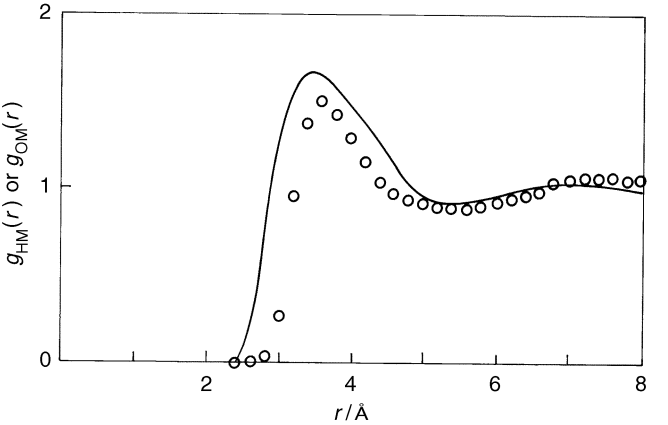

Fig. 7 The pair distribution functions $g_{MO}(r)$ (open circles) and $g_{MH}(r)$ (full curve) for the protons of methane molecules (CH_4) and water molecules (H_2O) in an aqueous mixture of methane in water under pressure.[318]

soluble in water and also exhibit hydrophobicity in the formation of large hydration shells.[314] They comprise 'ideal systems' for theoretical and experimental studies of hydrophobicity.[315,316] By the use of pressure, it is possible to dissolve sufficient amounts of apolar molecules and determine the local coordination by NDIS. This has been successfully achieved for argon (^{N}Ar,^{36}Ar) in heavy water and methane (CH_4/CD_4) in water–heavy water mixtures[317,318] and the results confirm the existence of a relatively well defined near neighbour hydration shell (Fig. 7). For Ar there are *ca.* 16(2) water molecules in the range $2.2 \leq r/\text{Å} \leq 4.6$, and for methane there are 19(2) in the range $2.4 \leq r/\text{Å} \leq 5$. Of particular interest is the extent of the short-range order in these systems, and it is found that in both cases there is little evidence to suggest that the argon atom or methane molecule extends its influence beyond the first hydration shell. This observation conflicts with results from computer simulations which generally show the existence of a well defined second hydration shell.[319–321]

Of additional interest in the case of methane hydration is the observation that the water molecules are orientated tangentially around the CH_4 molecule. It will be of interest to discover how temperature influences the structure, and experiments are already in hand to investigate the $g(r)$ functions for methane in the range up to the critical temperature of water.

Non-aqueous electrolyte solutions

A small programme of research based on NDIS methods has been established on a few select non-aqueous electrolyte solutions. The main focus of attention has been to characterise the coordinating properties of ions such as Li^+, Ni^{2+} and Cl^- and to establish how coordination numbers in particular change (Table 8).

One of the first studies[322] was made in methanol solutions of nickel chloride where attention was focused on the coordination of Ni^{2+}. The results of an NDIS study which also involved the use of H_2O–D_2O mixtures was to show that the Ni^{2+} ion

Table 8 Structural properties of ions in non-aqueous electrolyte solutions

ion	*electrolyte*	*solvent*	$r_{IO}/\AA$	$r_{ID}/\AA$	n_I	*ref.*
Li^+	LiBr (16.7 mol kg^{-1})	[$^2H_4$]methanol (CD_3OD)	1.97(5)	—	3.0(5)	323
	LiI (22.0 mol kg^{-1})	[$^2H_4$]methanol (CD_3OD)	1.93(5)	—	1.8(5)	323
Ni^{2+}	$NiCl_2$ (1 mol kg^{-1})	methanol (CD_3OD–CD_3OH)	2.07(2)	2.62(2)	3.7	322
	$Ni(CF_3SO_3)_2$ (6.9 mol kg^{-1})	ethylene glycol ($DOCD_2CD_2OD$)	$[Ni(EG)_3]^{2+}$ complexation			325
	$Ni(CF_3SO_3)_2$ (0.9 mol kg^{-1})	glycerol ($DOCD_2CD(OD)CD_2OD$)	$[Ni(glycerol)_2]^{2+}$ complexation			
Cu^{2+}	$Cu(CF_3SO_3)_2$ (2.8 mol kg^{-1})	ethylene glycol ($DOCD_2CD_2OD$)	1.98(2)	—	4	324
			2.26(2)	—	2	
			$[Cu(EG)_3]^{2+}$ complexation			
Cl^-	LiCl (1.7 mol dm^{-3})	heavy water	2.29	3.24	5.8(5)	324
		[$^2H_4$]methanol	3.21(3)	2.21(3)	3.6(5)	324
		[$^2H_7$]*N*,*N*-dimethylformamide [$DOCN(CD_3)_2$]	—	2.85	6.8(5)	324
	NaCl (1 mol kg^{-1})	ethylene glycol ($DOCD_2CD_2OD$)	3.13(3)	2.14(3)	~4	327

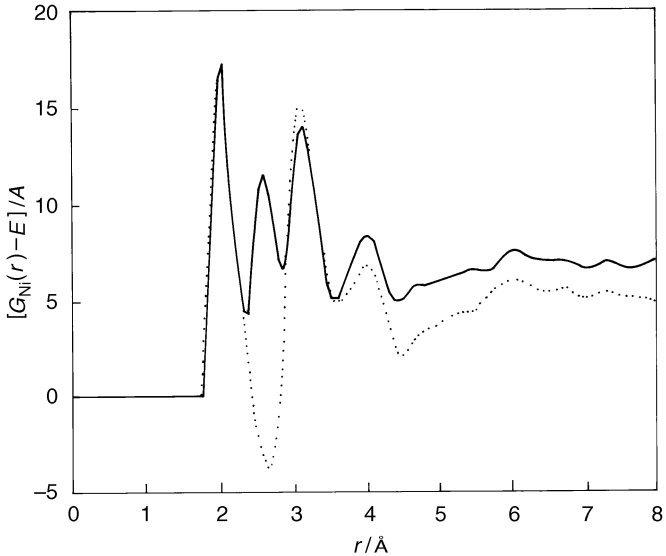

Fig. 8 The total Ni^{2+} pair distribution function $[G_{Ni}(r)–E]/A$ [eqn. (1)] in a 1 mol kg^{-1} solution of nickel chloride in methanol: $NiCl_2$ in CD_3OH (dotted curve); $NiCl_2$ in CD_3OD (full curve).[322]

coordinates strongly to the OH group of the CH_3OH molecule, with *ca.* 3.7 CH_3OH molecules and at least 0.8(3) Cl^- in the first coordination shell. There is also evidence to show that the second coordination shell of 9.5(1) methanol molecules penetrates significantly into the first shell (Fig. 8).

In a study of Li^+ coordination in highly concentrated solutions of lithium bromide (16.7 mol kg^{-1}) and lithium iodide (22 mol kg^{-1}) in methanol, Kameda *et al.*[323] showed that the Li^+ coordination is similarly altered from that in aqueous solution (Table 5). Although the distance between Li^+ and the oxygen of the nearest-neighbour methanol molecule is similar to that in aqueous solution, the coordination number is appreciably lower at 3.0(5) in LiBr and at 1.8(5) in LiI suggesting a substantial amount of cation–anion contact.

A parallel study of Cl^- in methanol and *N*,*N*-dimethylformamide (DMF) by the group of Yamaguchi,[324] shows that the coordination of Cl^- is also sensitive to solvent. Comparison of results (Table 8) shows that whereas the coordination number of Cl^- in water is *ca.* 6 it is slightly greater in DMF at *ca.* 7 and significantly smaller in methanol at 3.6(5), suggesting a strong degree of $Li^+ \cdots Cl^-$ association. The larger value of $\bar{n}_{Cl}^{DMF}$ for DMF is assumed to be due mostly to ion–dipole interactions.

In an attempt to understand the coordinating properties of the higher alcohols, Salmon and co-workers,[325–327] have embarked on NDIS studies of ionic coordination in glycerol ($DOCD_2CD(OD)CD_2OD$) and ethylene glycol (EG = $DOCD_2CD_2OD$). Using isotopes of Ni^{2+}, they showed that in nominally 1 mol kg^{-1} solutions of nickel sulfonate in fully deuteriated (EG), and in fully deuteriated glycerol, highly stable cation complexes are formed.[325] For the former, EG acts as a bidentate ligand to

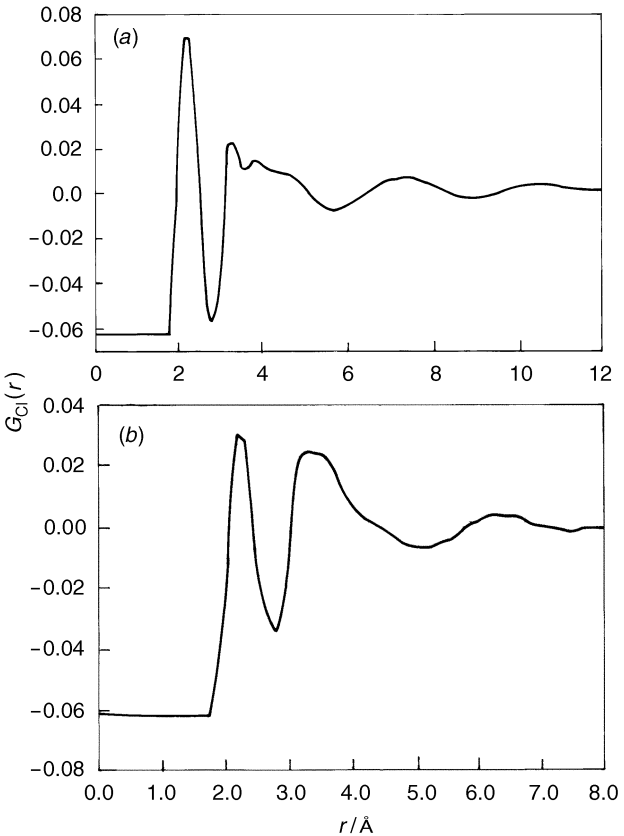

Fig. 9 The total pair distribution function $G_{cl}(r)$ for Cl^- anions in $LiCl{\cdot}4D_2O$: (*a*) glass at 120 K,[290,335] (*b*) liquid at 295 K.[292]

produce the tris-chelate species $[Ni(EG)_3]^{2+}$, and for the latter glycerol acts as a tridentate ligand to form $[Ni(glycerol)_2]^{2+}$. There is also no evidence of minor sphere complexing by the relatively weak sulfonate ion. A similar study of an ethylene glycol solution containing 2.8 mol kg^{-1} copper(II) triflate,[327] showed the presence of a Jahn–Teller distorted 4 + 2 coordination structure around the Cu^{2+} cation and the formation of tris-bidentate complexes $[Cu(EG)_3]^{2+}$. These results were also used to help understand the dynamics of these relatively large molecules in solution.

In a subsequent study of Cl^- coordination in 1 mol kg^{-1} sodium chloride in EG,[326] Salmon and Lond showed that the number of nearest neighbours is *ca.* 4, which is considerably less than the value of *ca.* 4 in sodium chloride in water.[253,254]

The above studies clearly demonstrate that the NDIS methods have wide-ranging applicability, and can be used to investigate how structure around ions depends on the dielectric nature of the solvent. Extension to second differences on the solute ions in, *e.g.*, $NiCl_2$ in methanol will facilitate a determination of $g_{++}(r)$, $g_{+-}(r)$ and $g_{--}(r)$ and

thereby provide a critical test of the dielectric influence on structure derived from primitive model (PM) calculations.[295,296,328]

Glasses and amorphous materials

The structure of non-crystalline materials can be studied by the same methods as used for liquids. Although the neutron formalism is slightly different for liquids and glasses the pair distribution function approach remains valid, and the use of isotopic substitution is equally effective.[329] Despite the obvious difference in the dynamical aspects of a liquid and glassy system, it is useful to know whether a structural distinction can be discerned between the two.

Amongst the many types of glasses we shall only focus on the results of electrolyte hydrates as an illustration of how NDIS methods can be used to elucidate the structure of a glass. The basic classification of these was undertaken by Angell and Sare,[330] who discovered that when plots were made of glassification temperature, T_g, as a function of ionic concentration there is a strong correlation with anion type. They also suggested that there could well be some form of structural signature which would readily distinguish the glass phase from the liquid.

The first neutron diffraction study of an aqueous electrolyte glass was undertaken by Dupuy *et al.*,[331] who determined the structural properties of lithium chloride in heavy water. Initial work was carried out at the total scattering level, where interesting but unresolved features are observed in the total structure functions. These experiments were followed up by more detailed NDIS studies of changes in water structure and Cl^- hydration when the system is glassified.[332] In the glass state of $LiCl{\cdot}6H_2O$ at 120 K it was found that differences in structure between the liquid and glass are minor. However, the equivalent structure in the supercooled liquid is appreciably different from that of the liquid at ambient conditions.[333] In a similar study of $LiCl{\cdot}4H_2O$ there is evidence to suggest that the water structure is no more disrupted on glassification than it is in the hexahydrate.[334]

Studies of anion hydration structure in $LiCl{\cdot}6D_2O$ show that the nearest-neighbour correlation is more pronounced in the glass; $G_{ClD}(r)$ exhibits a steep minimum at *ca.* 2.8 Å. This observation has recently been confirmed by Ansell *et al.*[335] in an NDIS study of the tetrahydrate (Fig. 9). Their measurements included an investigation of Li^+ coordination and at a deeper level the solute structure of the Cl^- ions in terms of $g_{ClCl}(r)$. As might be anticipated the results show that the Li^+ hydration shell is much sharper in the glass than in the liquid. Analysis of $g_{ClCl}(r)$ shows that there is an appreciable increase in the nearest neighbour coordination number over that in the liquid, 3.6(5) as opposed to 2.3(3), which suggests a greater degree of association between Cl^- and water molecules in the glass.

Neutron diffraction and NDIS studies have also been carried out on a wide variety of other glass systems, including those produced by rapid quenching, vapour deposition on to a cold surface or melt spinning followed by vapour deposition. Information on such diverse materials as metallic glasses, semiconductor glasses, silicates *etc.* can be found in the Annual Reports published by the various neutron laboratories such as ILL, ISIS, IPNS, SACLAY, KENS, *etc.*

For amorphous systems the work of Skipper and colleagues attests to the universal applicability of NDIS to study primary structure in condensed matter systems. In a series of studies on ionic coordination in vermiculite clays,[336–339] a system of both

biological and geological significance, NDIS results clearly demonstrate that in the confined region between the platelets, intercalated Ca^{2+} cations possess a well defined six-fold hydration shell similar to that found around cations such as Hg^{2+} and Cd^{2+}, and Ca^{2+} in concentrated $CaCl_2$ aqueous solutions. It is felt that this observation may be helpful in the explanation of 'how heavy ions can act as poisons in physiological processes'.[336]

A follow-up study of Li^+ hydration in vermiculite clays,[337] shows that whereas the larger alkali metal ions sodium, potassium and caesium tend to bind directly to the clay surface, Li^+ retains a six-fold hydration shell and remains solvent separated from the surface.

Complementary NDIS studies of the interlayer water structure in vermiculite clays containing sodium ions show a highly structured water network with strong hydrogen bonding between the water molecules and the clay surface.[338,339] As might be expected this result has important implications for studies of water structure in confined geometries.

3 Summary and future work

The above examples serve to illustrate the extent to which neutron diffraction isotopic substitution methods have been used to determine interatomic structure in a wide range of liquid and amorphous systems. The direct determination of pair radial functions not only offers a means of characterising the different structures in liquids, but also provides theorists with information to construct more realistic model potentials which can be used to explore properties in regimes not currently accessible to experiment.

It is anticipated that the NDIS methods will continue to be developed and applied to a wider range of systems. The construction and commissioning of new diffractometers with higher count rates, such as D20 and D4C at ILL, and GEM at ISIS with an optimised sample environment for work at non-ambient conditions, will enable new and more extensive research to be undertaken. Besides the many problems of immediate interest suggested at the end of some sections, there are several investigations which will become feasible in the longer term as the technology develops. These include: (i) the use of isotopes such as ^{12}C and ^{13}C, which will enable detailed and extensive structural studies to be carried out on a wide range of biologically significant materials, and (ii) the exploitation of higher count rates to investigate changes of structure as a chemical reaction occurs.

4 Acknowledgements

We thank our many colleagues to whose work we have referred in the preceding pages. We are particularly grateful to Dr. Barnes for his useful comments on the manuscript and its contents, Dr. Alan Soper for suggestions on the presentation of results on water and aqueous solutions, Dr. Chris Wormald for his help and expert advice on our molecular liquids, and Professor John Enderby for his enthusiastic support and insightful comments on many of the neutron results. We acknowledge our co-workers,

Drs. Stuart Ansell, Ian Howell, Paul deJong, R. Hans Tromp, John Wilson, Prof. Ryuzo Takagi (TIT, Japan) and Prof. Marcelle Gaune-Escard (IUSTI, France), and thank them for access to unpublished and about-to-be published results. We also thank our colleagues at the neutron institutions where many of the experiments were carried out. In particular, the services of Drs. Pierre Chieux and Henry Fischer (ILL), Marie Claire Bellissent Funel (LLB, Saclay), and Drs. Spenser Howells and Alan Soper (ISIS) have been essential to the success of most of the experiments described above. Finally we thank the SERC (now the EPSRC) for the continuing support of the many neutron programmes directed at the elucidation of liquid structure.

References

1 P. A. Egelstaff, *An Introduction to the Liquid State*, Oxford University Press, Oxford, 1992.
2 J. E. Enderby, in *Physics of Simple Liquids*, ed. H. N. V. Temperley, J. S. Rowlinson and G. S. Rushbrooke, North Holland, Amsterdam, 1968, ch. 14.
3 G. W. Neilson and J. E. Enderby, *J. Phys. Chem.*, 1996, **100**, 1317.
4 H. Ohtaki and T. Radnai, *Chem. Rev.*, 1993, **93**, 1157.
5 T. Yamaguchi, M. Namura, H. Wakita and H. Ohtaki, *J. Chem. Phys.*, 1988, **89**, 5153.
6 K. F. Ludwig Jr., W. K. Warburton, L. Wilson and A. I. Bienenstock, *J. Chem. Phys.*, 1987, **87**, 104.
7 K. Heinzinger, in *Computer Modelling of Fluids, Polymers and Solids*, ed. C. R. A. Catlow, S. C. Parker and M. P. Allen, Kluwer, Dordrecht, 1990, p. 357.
8 H. L. Friedman, *A Course in Statistical Mechanics*, Prentice Hall, New Jersey, 1985.
9 H. R. Glyde, *Excitations in Liquid and Solid Helium*, Oxford University Press, London, 1995.
10 J. E. Enderby and A. C. Barnes, *Rep. Prog. Phys.*, 1990, **53**, 85.
11 S. R. Elliott, *Physics of Amorphous Materials*, 2nd edn, Longman Scientific, New York, 1990.
12 V. F. Sears, *Neutron News*, 1992, **3**, 26.
13 T. E. Faber and J. M. Ziman, *Philos. Mag.*, 1964, **11**, 153.
14 K. Singer, A. Taylor and J. V. L. Singer, *Mol. Phys.*, 1977, **33**, 1757.
15 C. S. Murthy, K. Singer and I. R. McDonald, *Mol. Phys.*, 1981, **44**, 135.
16 O. Steinhauser and H. Bertagnolli, *Chem. Phys. Lett.*, 1981, **80**, 89.
17 H. J. Bohm, C. Meissner and R. Ahlrichs, *Mol. Phys.*, 1984, **53**, 651.
18 S.-B. Zhu, J. Lee and G. W. Robinson, *Mol. Phys.*, 1988, **65**, 65.
19 S.-B. Zhu and G. W. Robinson, *Comput. Phys. Commun.*, 1989, **52**, 317.
20 P. M. Roger, A. J. Stone and D. J. Tildesley, *J. Chem. Soc., Faraday Trans.* 2, 1987, **83**, 1689; *Mol. Phys.*, 1988, **63**, 173; *Chem. Phys. Lett.*, 1988, **145**, 365.
21 P. A. Madden and D. J. Tildesley, *Mol. Phys.*, 1981, **42**, 1137.
22 P. A. Madden and D. J. Tildesley, *Mol. Phys.*, 1983, **48**, 129.
23 K. E. Gubbins, C. G. Gray, P. A. Egelstaff and M. S. Ananth, *Mol. Phys.*, 1973, **25**, 1353.
24 L. J. Lowden and D. Chandler, *J. Chem. Phys.*, 1974, **61**, 5228.
25 H. C. Anderson, J. D. Weeks and D. Chandler, *Phys. Rev. A*, 1971, **4**, 1597.
26 J. B. van Tricht, H. Fredrikze and J. van der Laan, *Mol. Phys.*, 1984, **52**, 115.
27 T. Bausenwein, H. Bertagnolli, K. Todheide and P. Chieux, *Ber. Bunsenges. Phys. Chem.*, 1991, **95**, 577.
28 T. Bausenweim, H. Bertagnolli, D. Gutwerk, K. Todheide and P. Chieux, *Mol. Phys.*, 1992, **76**, 127.
29 G. Strauss, H. Zweier, H. Bertagnolli, T. Bausenwein, K. Todheide and P. Chieux, *J. Chem. Phys.*, 1994, **101**, 662.
30 W. A. Steele and S. I. Sandler, *J. Chem. Phys.*, 1974, **61**, 1315.
31 S. I. Sandler, A. Das Gupta and W. A. Steele, *J. Chem. Phys.*, 1974, **61**, 1326.
32 A. Das Gupta, S. I. Sandler and W. A. Steele, *J. Chem. Phys.*, 1975, **62**. 1769.
33 A. K. Adya and C. J. Wormald, *Mol. Phys.*, 1991, **74**, 735.
34 S. Chiappini, M. Nardone, F. P. Ricci and M. C. Bellissent-Funel, *Mol. Phys.*, 1997 (in press).
35 J. G. Powles, *Adv. Phys.*, 1973, **22**, 1.
36 L. Blum and A. H. Narten, *Adv. Chem. Phys.*, 1976, **34**, 203.
37 A. K. Adya and C. J. Wormald, *Mol. Phys.*, 1992, **77**, 1217.
38 P. A. Egelstaff, D. I. Page and J. G. Powles, *Mol. Phys.*, 1971, **20**, 881.
39 J. H. Clarke, J. C. Dore, G. Walford and R. N. Sinclair, *Mol. Phys.*, 1976, **31**, 883.
40 C. van der Marel, W. Bras and W. van der Lugt, *Mol. Phys.*, 1988, **64**, 445.
41 M. C. Bellissent-Funel, U. Buontempo, C. Petrillo and F. P. Ricci, *Mol. Phys.*, 1990, **71**, 253.
42 M. Zoppi, R. Magli, W. S. Howells and A. K. Soper, *Phys. Rev. A*, 1989, **39**, 4684.

43 M. Zoppi, U. Bafile, R. Magli and A. K. Soper, *Phys. Rev. E*, 1993, **48**, 1000.
44 M. Zoppi, U. Bafile, R. Magli and A. K. Soper, *J. Mol. Struct*., 1993, **296**, 243.
45 J. C. Dore, G. Walford and D. I. Page, *Mol. Phys*., 1975, **29**, 565.
46 J. H. Clarke, J. C. Dore and R. N. Sinclair, *Mol. Phys*., 1975, **29**, 581.
47 J. H. Clarke, J. C. Dore and H. Egger, *Mol. Phys*., 1980, **39**, 533.
48 P. A. Egelstaff and A. K. Soper, *Mol. Phys*., 1980, **40**, 569.
49 D. I. Page and J. G. Powles, *Mol. Phys*., 1971, **21**, 901.
50 J. G. Powles, J. C. Dore and E. K. Osae, *Mol. Phys*., 1980, **40**, 193.
51 J. G. Powles, J. C. Dore and E. K. Osae, *Mol. Phys*., 1980, **41**, 475.
52 J. D. Sullivan and P. A. Egelstaff, *Mol. Phys*., 1980, **39**, 329.
53 J. D. Sullivan and P. A. Egelstaff, *Mol. Phys*., 1981, **44**, 298.
54 M. Deraman, J. C. Dore and J. G. Powles, *Mol. Phys*., 1984, **52**, 173.
55 P. A. Egelstaff, R. K. Hawkins, D. Litchinsky, B. A. de Longi and J. B. Suck, *Mol. Phys*., 1984, **53**, 389.
56 C. Andreani, F. Cilloco and E. K. Osae, *Mol. Phys*., 1986, **57**, 931.
57 J. D. Sullivan and P. A. Egelstaff, *J. Chem. Phys*., 1982, **76**, 4631.
58 J. D. Sullivan and P. A. Egelstaff, *Chem. Phys*., 1983, **82**, 479.
59 P. Bosi, F. Cilloco, F. P. Ricci and F. Sacchetti, *Mol. Phys*., 1983, **49**, 567.
60 J. D. Sullivan and P. A. Egelstaff, *Chem. Phys*., 1984, **89**, 167.
61 M. C. Bellissent-Funel, U. Buontempo, C. Petrillo and F. P. Ricci, *Mol. Phys*., 1991, **74**, 1209.
62 G. Cagliotti and F. P. Ricci, *Nuovo Cimento*, 1962, **23**, 103.
63 P. Ascarelli and G. Cagliotti, *Nuovo Cimento*, 1966, **43**, 375.
64 R. W. Grubel and G. T. Clayton, *J. Chem. Phys*., 1967, **47**, 175.
65 M. Misawa, Y, Fukushima, K. Suzuki and S. Takeuchi, *Phys. Lett. A*. 1973, **45**, 273.
66 G. W. Stanton, J. H. Clarke and J. C. Dore, *Mol. Phys*., 1977, **34**, 823.
67 M. Misawa, *J. Chem. Phys*., 1989, **90**, 6563.
68 C. Andreani, F. Cilloco, L. Nencini, D. Rocca and R. N. Sinclair, *Mol. Phys*., 1985, **55**, 887.
69 P. Bisanti and F. Sacchetti, *Mol. Phys*., 1985, **54**, 255.
70 A. Filabozzi, U. Buontempo, R. Delaplane and F. P. Ricci, *Mol. Phys*., 1994, **82**, 427.
71 P. Bosi, F. Cilloco and M. A. Ricci, *Mol. Phys*., 1980, **40**, 1285.
72 C. Andreani, M. C. Bellissent-Funel, F. P. Ricci and M. A. Ricci, *Phys. Rev. A*., 1991, **44**, 5018.
73 M. Deraman, J. C. Dore, J. G. Powles, J. H. Holloway and P. Chieux, *Mol. Phys*., 1985, **55**, 1351.
74 A. K. Soper and P. A. Egelstaff, *Mol. Phys*., 1980, **39**, 1201.
75 A. K. Soper and P. A. Egelstaff, *Mol. Phys*., 1981, **42**, 399.
76 J. G. Powles, E. K. Osae, J. C. Dore and P. Chieux, *Mol. Phys*., 1981, **43**, 1051.
77 P. A. Egelstaff and A. K. Soper, *Mol. Phys*., 1980, **40**, 553; 569.
78 D. Gutwerk, T. Bausenwein and H. Bertagnolli, *Ber. Bunsenges. Phys. Chem*., 1994, **98**, 920.
79 J. G. Powles, J. C. Dore, E. K. Osae, J. H. Clarke, P. Chieux and S. Cummings, *Mol. Phys*., 1981, **44**, 1131.
80 C. Andreani, F. Menzinger, M. A. Ricci, A. K. Soper and J. Dreyer, *Phys. Rev. B*., 1994, **49**, 3811.
81 A. K. Soper, C. Andreani and M. Nardone, *Phys. Rev. E*., 1993, **47**, 2598.
82 C. Andreani, M. Nardone, F. P. Ricci and A. K. Soper, *Phys. Rev. A*, 1992, **46**, 4709.
83 M. A. Howe, C. J. Wormald and G. W. Neilson, *Mol. Phys*., 1989, **66**, 847.
84 M. C. Bellissent-Funel, U. Buontempo, C. Petrillo and F. P. Ricci, *Mol. Phys*., 1990, **71**, 239.
85 R. Ishii, S. Okazaki, I. Okada, M. Furusaka, N. Watanabe, M. Misawa and T. Fukunaga, *Chem. Phys. Lett*., 1995, **240**, 84.
86 R. Ishii, S. Okazaki, O. Odawara, I. Okada, T. Fukunaga and M. Misawa, *Fluid Phase Equilibria*, 1995, **104**, 291.
87 K. Suzuki and P. A. Egelstaff, *Can. J. Phys*., 1974, **52**, 241.
88 I. P. Gibson and J. C. Dore, *Mol. Phys*., 1981, **42**, 83.
89 J. B. van Tricht, G. H. Jansen and G. J. Davids, *J. Mol. Liq*, 1985, **31**, 91.
90 C. Andreani, V. Merlo, M. A. Ricci and A. K. Soper, *Mol. Phys*., 1991, **73**, 407.
91 T. Yamaguchi, O. Lindqvist and U. Dahlborg, *Acta Chem. Scand. Ser. A*, 1984, **38**, 757.
92 M. I. Cabaco, M. Besnard, M. C. Bellissent-Funel, Y. Guissani and B. Guillot, *Molecular Liquids*: *New Perspectives in Physics and Chemistry*, ed. J. J. C. Teixeira-Dias, Kluwer Dordrecht, 1992, p. 513.
93 M. I. Cabaco, Y. Danten, M. Besnard, M. C. Bellissent-Funel, Y. Guissani and B. Guillot, *Mol. Phys*., 1997 (in press).
94 M. I. Cabaco, Y. Danten, M. Besnard, Y. Guissani and B. Guillot, *Mol. Phys*., 1997 (in press).
95 M. Alvarez, F. J. Bermezo, W. S. Howells, E. Enciso, N. G. Almarza and M. Garciahernandez, *Mol. Phys*., 1990, **71**, 865.
96 H. Farman, J. C. Dore, M. C. Bellissent-Funel and D. G. Montague, *Mol. Phys*., 1987, **61**, 583.
97 H. Farman, F. Coveney, J. C. Dore and M. C. Bellissent-Funel, *Mol. Phys*., 1996, **87**, 1217.
98 E. Bartsch, H. Bertagnolli, G. Schulz and P. Chieux, *Ber. Bunsenges. Phys. Chem*., 1985, **89**, 147.
99 R. Felici, F. Cilloco and P. Bosi, *Mol. Phys*., 1990, **70**, 455.
100 M. Misawa and T. Fukunaga, *J. Chem. Phys*., 1990, **93**, 3495.
101 T. Matsumoto, *AIP Conference Proceedings*, 1982, **89**, 90.

102 H. Bertagnolli, I. Hummel and P. Chieux, *Ber. Bunsenges. Phys. Chem*., 1988, **92**, 1149.
103 M. Misawa and T. Fukunaga, *J. Chem. Phys*., 1990, **93**, 3495.
104 C. D. Hall, K. A. Johnson, A. N. Burgess, N. Winterton and W. S. Howells, *Mol. Phys*., 1991, **74**, 27.
105 C. D. Hall, K. A. Johnson, A. N. Burgess, N. Winterton and W. S. Howells, *Mol. Phys*., 1992, **76**, 1061.
106 M. I. Cabaco, Y. Danten, M. Besnard, Y. Guissani and B. Guillot, *Chem. Phys. Lett*, 1997 (in press).
107 W. G. Jung, M. D. Zeidler and P. Chieux, *Mol. Phys*., 1989, **68**, 473.
108 H. Bertagnolli, D. O. Leicht, M. D. Zeidler and P. Chieux, *Mol. Phys*., 1978, **35**, 193; 199.
109 H. Bertagnolli, D. O. Leicht, M. D. Zeidler and P. Chieux, *Mol. Phys*., 1978, **6**, 1769.
110 H. Bertagnolli and P. Chieux, *Ber. Bunsenges. Phys. Chem*., 1980, **84**, 1225.
111 H. Bertagnolli, *Ber. Bunsenges. Phys. Chem*., 1981, **85**, 644.
112 H. Bertagnolli and M. D. Zeidler, *J. Mol. Liq*., 1983, **25**, 277.
113 H. Bertagnolli and P. Chieux, *Mol. Phys*., 1984, **51**, 617.
114 J. H. Clarke, J. C. Dore, J. P. Gibson, J. R. Granada and G. W. Stanton, *Faraday Discuss. Chem. Soc*., 1978, **66**, 277.
115 J. R. Granada, G. W. Stanton, J. H. Clarke and J. C. Dore, *Mol. Phys*., 1979, **37**, 1297.
116 J. H. Clarke, J. R. Granada and J. C. Dore, *Mol. Phys*., 1979, **37**, 1263.
117 F. J. Bermejo, E. Eniso, J. Alonso, N. Garcia and W. S. Howells, *Mol. Phys*., 1988, **64**, 1169.
118 M. Misawa, *J. Chem. Phys*., 1989, **91**, 5648.
119 I. J. Bermejo, E. Enicso, J. C. Dore, P. Chieux, N. Garcia and J. Santoro, *J. Chem. Phys*., 1987, **87**, 7171.
120 M. Alvarez, F. J. Bermejo, W. S. Howells, P. Chieux, E. Enciso, J. Alonso and N. Garcia, *J. Chem. Phys*., 1989, **91**, 3689.
121 P. Zetterstrom, U. Dahlborg and A. Wannberg, *Mol. Phys*., 1994, **83**, 971.
122 H. Bertagnolli, T. Engelhardt and B. Lengeler, *Ber. Bunsenges. Phys. Chem*., 1987, **91**, 1287.
123 H. Bertagnolli, T. Engelhardt and P. Chieux, *Ber. Bunsenges. Phys. Chem*., 1988, **92**, 84.
124 I. P. Gibson and J. C. Dore, *Mol. Phys*., 1979, **37**, 1281.
125 D. G. Montague, I. P. Gibson and J. C. Dore, *Mol. Phys*., 1981, **44**, 1355.
126 D. G. Montague, J. C. Dore and S. Cummings, *Mol. Phys*., 1984, **53**, 1049.
127 Y. Tanaka, N. Ohtomo and K. Arakawa, *Bull. Chem. Soc. Jpn*., 1984, **57**, 644.
128 Y. Tanaka, N. Ohtomo and K. Arakawa, *Bull. Chem. Soc. Jpn*., 1985, **58**, 270.
129 D. G. Montague and J. C. Dore, *Mol. Phys*., 1986, **57**, 1035.
130 F. J. Bermejo, F. J. Nompean, J. Santoro, D. C. Steytler and J. C. Dore, *J. Mol. Liq*., 1987, **33**, 183.
131 F. J. Bermejo, F. Batallan, E. Enciso, M. Garciahernandez, J. Alonso and J. L. Martinez, *Euro. Phys. Lett*., 1990, **12**, 129.
132 F. J. Bermejo, F. Batallan, J. L. Martinez, M. Garciahernandez and E. Enciso, *J. Phys.: Condens. Matter*, 1990, **2**, 6659.
133 J. Alonso, F. J. Bermejo, M. Garciahernandez, J. L. Martinez, W. S. Howells and A. Criado, *J. Chem. Phys*., 1992, **96**, 7696.
134 D. G. Montague, I. P. Gibson and J. C. Dore, *Mol. Phys*., 1982, **47**, 1405.
135 Y. Tanaka, N. Ohtomo and K. Arakawa, *Bull. Chem. Soc. Jpn*., 1984, **57**, 2569.
136 P. Zetterstrom, U. Dahlborg, R. G. Delaplane and W. S. Howells, *Phys. Scr*., 1991, **44**, 56.
137 P. Zetterstrom, U. Dahlborg and W. S. Howells, *Mol. Phys*., 1994, **81**, 1187.
138 D. C. Champeney, R. N. Joarder and J. C. Dore, *Mol. Phys*., 1986, **58**, 337.
139 H. Bertagnolli and M. Hoffman, *Z. Phys. Chem. Neue Folge*, 1988, **159**, 185.
140 H. Bertagnolli, M. Hoffman and M. Ostheimer, *Z. Phys. Chem*., 1989, **165**, 165.
141 H. Bertagnolli, P. Chieux and H. G. Hertz, *Ber. Bunsenges Phys. Chem*., 1984, **88**, 977.
142 H. Bertagnolli and H. G. Hertz, *Ber. Bunsenges Phys. Chem*., 1985, **89**, 500.
143 P. Jedlovszky, I. Bako, G. Palinkas and J. C. Dore, *Mol. Phys*., 1995, **86**, 87.
144 H. Bertagnolli, *Chem. Phys. Lett*., 1982, **93**, 287.
145 P. Chieux and H. Bertagnolli, *J. Phys. Chem*., 1984, **88**, 3726.
146 T. Bausenwein, H. Bertagnolli, A. David, K. Goller, H. Zweier, K. Todheide and P. Chieux, *J. Chim. Phys*., 1994, **101**, 672.
147 M. A. Ricci, M. Nardone, F. P. Ricci, C. Andreani and A. K. Soper, *J. Chem. Phys*., 1995, **102**, 7650.
148 H. Bertagnolli and K. Todheide, *J. Phys.: Condens. Matter*, 1996, **8**, 9293.
149 J. B. van Tricht, H. W. van Zeyl and P. van derende, *J. Mol. Liq*., 1988, **38**, 97.
150 M. Misawa, T. Fukunaga and K. Suzuki, *J. Chem. Phys*., 1990, **92**, 5486.
151 G. Walford, J. H. Clarke and J. C. Dore, *Mol. Phys*., 1978, **36**, 1581.
152 E. Kalman, I. Serke, G. Palinkas, M. D. Zeidler, F.J. Wiesmann, H. Bertagnolli and P. Chieux, *Z. Naturforsch., Teil A* 1983, **38**, 231.
153 F. J. Weismann, M. D. Zeidler, H. Bertagnolli and P. Chieux, *Mol. Phys*., 1986, **57**, 275.
154 J. Neuefeind, P. Chieux and M. D. Zeidler, *Mol. Phys*., 1992, **76**, 143.
155 H. Bertagnolli, P. Chieux and M. D. Zeidler, *Mol. Phys*., 1976, **32**, 759.
156 H. Bertagnolli, P. Chieux and M. D. Zeidler, *Mol. Phys*., 1976, **32**, 1731.
157 H. Bertagnolli, T. Engelhardt and P. Chieux, *Ber. Bunsenges. Phys. Chem*., 1986, **90**, 512.
158 H. Bertagnolli, E. Schultz and P. Chieux, *Ber. Bunsenges. Phys. Chem*., 1989, **93**, 88.

159 A. Luzar and D. Chandler, *J. Chem. Phys.*, 1993, **98**, 8160.
160 A. Luzar, A. K. Soper and D. Chandler, *J. Chem. Phys.*, 1993, **99**, 6836.
161 A. K. Adya and C. J. Wormald, *Mol. Phys.*, 1993, **78**, 1075.
162 U. Mittag, J. Samios, T. Dorfmueller, S. Guenster, M. D. Zeidler and P. Chieux, *Mol. Phys.*, 1989, **67**, 1141.
163 E. Bartsch, H. Bertagnolli and P. Chieux, *Ber. Bunsenges. Phys. Chem.*, 1986, **90**, 34.
164 J. H. Clarke, J. C. Dore, I. P. Gibson, J. R. Granada and G. W. Stanton, *Faraday Discuss. Chem. Soc.*, 1978, **66**, 277.
165 E. Enciso, M. Lombardero and J. C. Dore, *Mol. Phys.*, 1986, **59**, 941.
166 A. K. Soper and A. Luzar, *J. Chem. Phys.*, 1992, **97**, 1320.
167 C. Andreani, J. C. Dore and F. P. Ricci, *Rep. Prog. Phys.*, 1991, **54**, 731.
168 M. A. Howe, *Mol. Phys.*, 1990, **69**, 161.
169 D. G. Pritchard, R. N. Nandi, J. S. Muenter and B. J. Howard, *J. Chem. Phys.*, 1988, **89**, 1245.
170 J. E. Enderby, D. M. North and P. A. Egelstaff, *Philos. Mag.*, 1966, **14**, 961.
171 D. I. Page and K. Mika, *J. Phys. C.*, 1971, **4**, 3034.
172 F. G. Edwards, J. E. Enderby, R. A. Howe and D. I. Page, *J. Phys. C.*, 1975, **8**, 3483.
173 S. Biggin and J. E. Enderby, *J. Phys. C.*, 1981, **14**, 3129.
174 D. A. Allen, R. A. Howe, N. D. Wood and W. S. Howells, *J. Phys. Conden. Matter*, 1992, **4**, 1407.
175 A. K. Adya and G. W. Neilson, *Mol. Phys.*, 1990, **69**, 747.
176 A. K. Adya, G. W. Neilson, I. Okada and S. Okazaki, *Mol. Phys.*, 1993, **79**, 1327.
177 A. K. Adya and G. W. Neilson, *Mol. Phys.*, 1990, **71**, 1091.
178 A. K. Adya, R. Takagi, Y. Sato, M. Gaune-Escard, H. Fischer and A. C. Barnes, *J. Chem. Phys.*, 1997 (to be published).
179 L. V. Woodcock and K. Singer, *Trans. Faraday Soc.*, 1971, **67**, 12.
180 M. Dixon and M. J. L. Sangster, *J. Phys. C.*, 1975, **8**, L8; 1976, **9**, L5; 1976, **9**, 909.
181 H. V. Wechem, *Doctoral Thesis*, University of Amsterdam, 1976.
182 L. V. Woodcock, C. A. Angell and P. Cheeseman, *J. Chem. Phys.*, 1976, **65**, 1565.
183 S. de Leeuw, *Mol. Phys.*, 1978, **36**, 103; 765.
184 M. Dixon and M. J. Gillan, *Philos. Mag. Sect. B*, 1981, **43**, 1099.
185 R. L. McGreevy and E. W. J. Mitchell, *J. Phys. C.*, 1982, **15**, 5537.
186 M. L. Saboungi, A. Rahman and M. Blander, *J. Chem. Phys.*, 1984, **80**, 2141.
187 P. J. Gardner and D. M. Heyes, *Physica B*, 1985, **113**, 227.
188 G. Pastore, P. Ballone and M. P. Tosi, *J. Phys. C.*, 1986, **19**, 487.
189 T. Yamaguchi, I. Okada, H. Ohtaki, M. Mikami and K. Kawamura, *Mol. Phys.*, 1986, **58**, 349.
190 A. K. Adya, R. Takagi, K. Kawamura and M. Mikami, *Mol. Phys.*, 1987, **62**, 227.
191 M. Wilson and P. A. Madden, *J. Phys.: Condens. Matter*, , 1993, **5**, 6833; 1994, **6**, 159.
192 R. Takagi, L. Rycerz and M. Gaune-Escard, *Denki Kagaku*, 1994, **62**, 240.
193 L. Koester, K. Knopf and K. Waschkowski, *Z. Phys., Teil A.*, 1977, **282**, 371.
194 M. A. Howe and R. L. McGreevy, *Philos. Mag. Sect. B.*, 1988, **58**, 485.
195 J. C. Li, J. M. Titman, G. E. Carr, N. Cowlam and J. B. Suck, *Physica B*, 1989, **156**, 168.
196 R. L. McGreevy and M. A. Howe, *J. Phys.: Condens. Matter*, 1989, **1**, 9957.
197 H. A. Levy, P. A. Agron, M. A. Bredig and M. D. Danford, *Ann. N Y Acad. Sci.*, 1960, **79**, 762.
198 S. Biggin and J. E. Enderby, *J. Phys. C.*, 1982, **15**, L305.
199 H. Ohno and K. Furukawa, *J. Chem. Soc., Faraday Trans. 1*, 1981, **77**, 1981.
200 J. Y. Derrien and J. Dupuy, *J. Phys. Paris*, 1975, **36**, 191.
201 E. W. J. Mitchell, P. F. J. Poncet and R. J. Stewart, *Philos. Mag, Sect. B*, 1976, **34**, 721.
202 J. Locke, S. Messoloras, R. J. Stewart, R. L. McGreevy and E. W. J. Mitchell, *Philos. Mag., Sect. B*, 1985, **51**, 301.
203 S. Eisenberg, J.-F. Jal, J. Dupuy, P. Chieux and W. Knoll, *Philos. Mag., Sect. A*, 1982, **46**, 195.
204 J. Y. Derrien and J. Dupuy, *Phys. Chem. Liq.*, 1976, **5**, 71.
205 D. A. Allen and R. A. Howe, *J. Phys.: Condens. Matter*, 1992, **4**, 6029.
206 R. Trioli and A. H. Narten, *J. Chem. Phys.*, 1981, **74**, 703.
207 D. A. Allen, R. A. Howe, N. D. Wood and W. S. Howells, *J. Chem. Phys.*, 1991, **94**, 5071.
208 S. Biggin, M. Gay and J. E. Enderby, *J. Phys. C*, 1984, **17**, 977.
209 H. Ohno, K. Furukawa, K. Tanemoto, Y. Takagi and T. Nakamura, *J. Chem. Soc., Faraday Trans. 1*, 1978, **74**, 804.
210 S. E. Day and R. L. McGreevy, *Phys. Chem. Liq.*, 1985, **15**, 129.
211 M. C. Fairbanks, M. A. Howe and R. L. McGreevy, *Phys. Chem. Liq.*, 1988, **18**, 179.
212 R. L. McGreevy, *Solid State Phys.*, 1987, **40**, 247.
213 S. Biggin and J. E. Enderby, *J. Phys. C.*, 1981, **14**, 3577.
214 F. G. Edwards, R. A. Howe, J. E. Enderby and D. I. Page, *J. Phys. C.*, 1978, **11**, 1053.
215 R. J. Newport, R. A. Howe and N. D. Wood, *J. Phys. C.*, 1985, **18**, 5249.
216 N. D. Wood and R. A. Howe, *J. Phys. C.*, 1988, **21**, 3177.
217 N. D. Wood, R. A. Howe, R. J. Newport and J. Faber Jr., *J. Phys. C.*, 1988, **21**, 669.
218 Y. S. Badyal and R. A. Howe, *J. Phys.: Condens. Matter*, 1993, **5**, 7189.

219 R. L. McGreevy and L. Pusztai, *Proc. R. Soc. London, Ser. A*, 1990, **430**, 241.
220 Y. S. Badyal, D. A. Allen and R. A. Howe, *J. Phys.: Condens. Matter*, 1994, **6**, 10 193.
221 R. L. Harris, R. E. Wood and H. L. Ritter, *J. Am. Chem. Soc.*, 1951, **73**, 3121.
222 Y. Fukushima, M. Misawa and K. Suzuki, *Res. Rep. Lab. Nucl. Sci.* (*Tohoku University*), 1975, **8**, 113.
223 M. L. Saboungi, M. A. Howe and D. L. Price, *Mol. Phys.*, 1993, **79**, 847.
224 P. S. Salmon, *Proc. R. Soc. London, Ser. A*, 1992, **437**, 591.
225 P. S. Salmon, *Proc. R. Soc. London, Ser. A*, 1994, **445**, 351.
226 Y. S. Badyal and R. A. Howe, *J. Phys.: Condens. Matter*, 1996, **8**, 3733.
227 S. Biggin, S. Cummings, J. E. Enderby and M. Blander, *Proc. Electrochem. Soc.*, 1986, **86**, 81.
228 M. Blander, E. Bierwagen, K. G. Calkins, L. A. Curtiss, D. L. Price and M. L. Saboungi, *J. Chem. Phys.*, 1992, **97**, 2733.
229 Y. Shirakawa, S. Tamakji, T. Usuki, K. Sugiyama and Y. Waseda, *J. Phys. Soc. Jpn.*, 1994, **63**, 1814.
230 Y. Shirakawa, M. Saito, S. Tamaki, M. Inui and S. Takeda, *J. Phys. Soc. Jpn.*, 1991, **60**, 2678.
231 M. Inui, S. Takeda, Y. Shirakawa, S. Tamaki, Y. Waseda and Y. Yamaguchi, *J. Phys. Soc. Jpn.*, 1991, **60**, 3025.
232 Y. Kameda, S. Kotani and K. Ichikawa, *Mol. Phys.*, 1992, **75**, 1.
233 R. W. G. Wyckoff, *Crystal Structures*, 2nd edn., Wiley Interscience, New York, vol. 2, 1964.
234 K. Suzuki and Y. Fukushima, *Z. Naturforsch., Teil A*, 1977, **32**, 1438.
235 T. Yamaguchi, Y. Tamura, I. Okada, H. Ohtaki, M. Misawa and N. Watanabe, *Z. Naturforsch., Teil A*, 1985, **40**, 490.
236 H. Ohno and K. Furukawa, *J. Chem. Soc., Faraday Trans.* 1, 1978, **74**, 297.
237 K. Furukawa and H. Ohno, *Busseiron Kenkyu*, 1973, **19**, 1335.
238 A. K. Adya and G. W. Neilson, *J. Chem. Soc., Faraday Trans. 1*, 1991, **87**, 279.
239 P. Andonov, P. Chieux and S. Kimura, *J. Phys.: Condens. Matter*, 1993, **5**, 4865.
240 A. K. Soper and J. Turner, *Int. J. Mol. Phys.*, 1993, **B7**, 3049.
241 A. K. Soper, *J. Chem. Phys.*, 1994, **101**, 6888.
242 L. Bosio, J. Texeira and M. C. Bellissent-Funel, *Phys. Rev. A.*, 1989, **39**, 6612.
243 M. C. Bellissent-Funel, in *Hydrogen Bonded Liquids*, ed. J. C. Dore and J. Teixeira, NATO ASI C329, Kluwer, Dordrecht, 1991, p. 117.
244 A. K. Soper, *J. Phys.: Condens. Matter*, 1996, **8**, 9263.
245 P. Postoroni, M. A. Ricci and A. K.Soper, *J. Chem. Phys.*, 1994, **101**, 4123.
246 A. K. Soper, F. Bruni and M. A. Ricci, *J. Chem. Phys.*, (in press).
247 R. H. Tromp, P. Postorini, G. W. Neilson, M. A. Ricci and A. K. Soper, *J. Chem. Phys.*, 1994, **101**, 6210.
248 A. A. Chialvo and P. T. Cummings, *J. Phys. Chem.*, 1996, **100**, 1309.
249 Y. Guissani and B. Giullot, *J. Chem. Phys.*, 1993, **98**, 8221.
250 A. Geiger, P. Mausbach and J. Schnitker, *Water and Aqueous Solutions*, ed. G. W. Neilson and J. E. Enderby, Adam Hilger, Bristol, 1985, p. 15.
251 A. H. Narten, P. Vaslow and H. A. Levy, *J. Chem. Phys.*, 1973, **58**, 5017.
252 J. E. Enderby and G. W. Neilson, *Water, a Comprehensive Treatise*, ed. F. Franks, Plenum Press, New York, 1979, vol. 6, ch. 1.
253 G. W. Neilson and J. E. Enderby, *J. Phys. Chem.*, 1996, **100**, 1317.
254 G. W. Neilson and R. H. Tromp, *Annu. Rep. Prog. Chem., Sect. C*, 1991, 185.
255 D. H. Powell, G. W. Neilson and J. E. Enderby, *J. Phys: Condens. Matter*, 1993, **5**, 5723.
256 M. Sprik, M. L. Klein and K. Wanabe, *J. Phys. Chem.*, 1990, **94**, 6483.
257 L. X. Dang, J. E. Rice, J. Caldwell and P. A. Kollman, *J. Am. Chem. Soc.*, 1991, **113**, 2481.
258 I. Howell and G. W. Neilson, *J. Phys.: Condens. Matter*, 1996, **8**, 4455.
259 W. Rudolph, M. H. Brooker and C. C. Pye, *J. Phys. Chem.*, 1995, **99**, 3793.
260 N. A. Hewish and G. W. Neilson, *Chem. Phys. Lett.*, 1981, **84**, 425.
261 G. W. Neilson and N. T. Skipper, *Chem. Phys. Lett.*, 1985, **114**, 35.
262 N. A. Hewish, G. W. Neilson and J. E. Enderby, *Nature* (*London*), 1982, **297**, 138.
263 R. D. Broadbent, G. W. Neilson and M. Sandström, *J. Phys.: Condens. Matter*, 1992, **4**, 639.
264 G. J. Herdman and G. W. Neilson, *J. Phys.: Condens. Matter*, 1992, **4**, 649.
265 G. J. Herdman and G. W. Neilson, *J. Phys.: Condens. Matter*, 1992, **4**, 627.
266 D. H. Powell and G. W. Neilson, *J. Phys.: Condens. Matter*, 1990, **2**, 3871.
267 J. R. Newsome, G. W. Neilson, J. E. Enderby and M. Sandström, *Chem. Phys. Lett.*, 1981, **82**, 399.
268 P. S. Salmon, G. W. Neilson and J. E. Enderby, *J. Phys. C.*, 1988, **21**, 1335.
269 P. S. Salmon and G. W. Neilson, *J. Phys.: Condens. Matter*, 1989, **1**, 529.
270 D. H. Powell, P. M. N. Gullidge, M. C. Bellissent-Funel and G. W. Neilson, *Mol. Phys.*, 1990, **71**, 1107.
271 M. Sandström, G. W. Neilson, G. Johansson and T. Yamaguchi, *J. Phys. C*, 1985, **18**, L1115.
272 A. H. Narten and R. L. Hahn, *J. Phys. Chem.*, 1983, **87**, 3193.
273 B. K. Annis, R. L. Hahn and A. H. Narten, *J. Chem. Phys.*, 1985, **82**, 2086.
274 C. Cossy, A. C. Barnes, J. E. Enderby and A. E. Merbach, *J. Chem. Phys.*, 1989, **90**, 3254.
275 G. W. Neilson, D. Schiöberg and W. A. P. Luck, *Chem. Phys. Lett.*, 1985, **122**, 475.
276 Y. Kameda, H. Arakawa, K. Hamgai and O. Uemura, *Bull Chem. Soc. Jpn.*, 1992, **65**, 2154.

277 Y. Kameda, H. Saitoh and O. Uemura, *Bull. Chem. Soc. Jpn*., 1993, **66**, 1919.
278 Y. Kameda, H. Arakawa, K. Haugai and O. Uemura, *Bull. Chem. Soc. Jpn*., 1994, **67**, 956.
279 See *e.g*. J. M. H. Levelt Sengers in *Physical Chemistry of Aqueous Systems*, ed. H. J. White Jr, J. V. Sengers, D. B. Neumann and J. C. Bellows, Begell House, New York, 1995.
280 G. W. Neilson, R. D. Broadbent, M. A. Howe and E. U. Franck, in *Properties of Water and Steam*, ed. M. Pichal and O. Sifner, Hemisphere, New York, 1990, p. 335.
281 P. H. K. de Jong, G. W. Neilson and M. C. Bellissent-Funel, *J. Chem. Phys*., 1996, **105**, 5155.
282 I. Howell and G. W. Neilson, *J. Chem. Phys*., 1996, **104**, 2036.
283 T. Yamaguchi, M. Yamagami, H. Ohzano, H. Wakita and K. Yamanaka, *Chem. Phys. Lett*., 1996, **252**, 317.
284 T. Yamaguchi, M. Yamagami, H. Ohzano, K. Yamanaka and H. Wakita, *Physica B*, 1995, **213**/**214**, 480.
285 R. H. Tromp, G. W. Neilson and A. K. Soper, *J. Chem. Phys*., 1992, **96**, 8460.
286 J. L. Finney, J. Turner and A. K. Soper, *Mol. Phys*., 1992, **77**, 411.
287 P. H. K. de Jong and G. W. Neilson, *J. Phys.: Condens. Matter*, 1996, **8**, 9275.
288 R. Leberman and A. K. Soper, *Nature* (*London*), 1995, **378**, 364.
289 K. D. Collins and M. W. Washabaugh, *Q. Rev. Biophys*., 1985, **18**, 323.
290 S. Ansell, *Ph.D. Thesis*, University of Bristol, 1995; S. Ansell and G. W. Neilson, in preparation.
291 S. Ansell, R. H. Tromp and G. W. Neilson, *J. Phys.: Condens. Matter*, 1995, **7**, 1513.
292 I. Howell, *Ph.D. Thesis*, University of Bristol; I. Howell and G. W. Neilson, *J. Mol. Liq*. (submitted).
293 G. W. Neilson and J. E. Enderby, *Proc. R. Soc. London, Ser. A*, 1983, **390**, 353.
294 N. T. Skipper, G. W. Neilson and S. Cummings, *J. Phys.: Condens. Matter*, 1989, **1**, 3489.
295 H. L. Friedman, *Faraday Discuss. Chem. Soc*., 1988, **85**, 1.
296 J. E. Enderby and G. W. Neilson, *Adv. Phys*., 1980, **29**, 323.
297 J. R. C. van der Maarel, D. H. Powell, A. L. Jawahier, L. H. Leyte-Zuiderweg, G. W. Neilson and M. C. Bellissent-Funel, *J. Chem. Phys*., 1989, **90**, 670.
298 R. H. Tromp and G. W. Neilson, *J. Phys. Chem*., 1996, **100**, 7380.
299 R. H. Tromp, G. W. Neilson and M. C. Bellissent-Funel, *J. Phys. Chem*., 1994, **98**, 13 195.
300 T. W. N. Beize, R. H. Tromp. J. R. C. van der Maarel, M. H. J. M. van Strien, M. C. Bellissent-Funnel, G. W. Neilson and J. C. Leyte, *J. Phys. Chem*., 1994, **98**, 4454.
301 T. W. Beize, A. C. Barnes, C. J. M. Huige and J. C. Leyte, *J. Phys. Chem*., 1994, **98**, 6568.
302 J. E. Wilson, S. Ansell, J. E. Enderby and G. W. Neilson, *Structure around chloride ions in the presence of biological macromolecules*, manuscript in preparation.
303 J. Turner, J. L. Finney, J. P. Bouquiere, G. W. Neilson, S. Cummings and J. Bouillot, in *Water and Aqueous Solutions*, ed. G. W. Neilson and J. E. Enderby, Adam Hilger, Bristol, 1996, p. 277.
304 J. L. Finney, in *Water and Aqueous Solutions*, ed. G. W. Neilson and J. E. Enderby, Adam Hilger, Bristol, 1986, p. 227.
305 J. L. Finney, A. K. Soper and J. Turner, *Physica B*., 1989, **156**/**157**, 151.
306 R. A. Kuharshi and P. J. Rossky, *J. Am. Chem. Soc*., 1984, **106**, 5786.
307 J. Z. Turner, A. K. Soper and J. L. Finney, *J. Chem. Phys*., 1995, **102**, 5438.
308 J. L. Finney and J. Turner, *Faraday Discuss. Chem. Soc*., 1988, **85**, 125.
309 A. K. Soper and J. L. Finney, *Phys. Rev. Lett*., 1993, **71**, 4346.
310 A. K. Soper and A. Luzar, *J. Phys. Chem*., 1996, **100**, 1357.
311 E. C. Hulme, A. K. Soper, J. L. Finney, *The Hydration of Acetylcholine in Aqueous Solution*, to be published.
312 P. M. N. Gullidge and G. W. Neilson, *Chem. Phys. Lett*., 1990, **165**, 457.
313 R. K. Gupta and A. Mildvan, *J. Biol. Chem*., 1977, **252**, 5967.
314 R. Crovetto, R. Fernandez-Prini and M. L. Japas, *J. Chem. Phys*., 1982, **76**, 1077.
315 D. W. Davidson, in *Water, a Comprehensive Treatise*, ed. F. Franks, Plenum Press, New York, 1973, vol. 2, ch. 3.
316 W. Blokzyjl and J. B. F. N. Eugberts, *Angew. Chem., Int. Ed. Engl*., 1993, **32**, 1545.
317 R. D. Broadbent and G. W. Neilson, *J. Chem. Phys*., 1994, **100**, 7543.
318 P. H. K. de Jong, J. E. Wilson, G. W. Neilson and A. D. Buckingham, *Mol. Phys*., (in press).
319 C. Pangali, M. Rao and B. J. Berne, *J. Chem. Phys*., 1979, **71**, 2975.
320 L. R. Pratt, *Annu. Rev. Phys. Chem*., 1985, **36**, 433.
321 B. Guillot and Y. Guissani, *J. Chem. Phys*., 1993, **99**, 8075.
322 D. H. Powell and G. W. Neilson, *J. Phys.: Condens. Matter*, 1990, **2**, 5867.
323 Y. Kameda, H. Ebata, T. Usuki and O. Vermura, *Physica B*., 1995, **213**/**214**, 477.
324 M. Yamagami, H. Wakita and T. Yamaguchi, *J. Chem. Phys*., 1995, **103**, 8174.
325 S. E. Okan, P. S. Salmon, D. C. Champaney and I. Petri, *Mol. Phys*., 1995, **84**, 325.
326 P. S. Salmon and P. B. Lond, *J. Phys.: Condens. Matter*, 1992, **4**, 5349.
327 S. E. Okan and P. S. Salmon, *Mol. Phys*., 1995, **85**, 981.
328 J. C. Rasaiah and H. L. Friedman, *J. Chem. Phys*., 1968, **48**, 2742.
329 A. J. Leadbetter, in *Chemical Applications of Thermal Neutron Scattering*, ed. B. T. M. Willis, Oxford University Press, London, 1973, ch. 7.
330 C. A. Angell and E. J. Sare, *J. Chem. Phys*., 1970, **52**, 1058.
331 J. Dupuy, A. Elarby-Aouizerat, P. Claudy, J.-F. Jal, J. M. Letoffe and P. Chieux, in *Aqueous Ionic Solutions*,

ed. M. C. Bellissent-Funel and G. W. Neilson, NATO ASI C205, Reidel, Dordrecht, 1987, p. 447.
332 S. Prevel, J.-F. Jal, J. Dupuy-Philon and A. K. Soper, *J. Chem. Phys*., 1995, **103**, 1886.
333 S. Prevel, J.-F. Jal, J. Dupuy-Philon and A. K. Soper, *J. Chem. Phys*., 1995, **103**, 1897.
334 J.-F. Jal, A. K. Soper, P. Carmona and J. Dupuy, *J. Phys.: Condens. Matter*, 1991, **3**, 551.
335 S. Ansell, J. Dupuy, J.-F. Jal and G. W. Neilson, *Ionic structure in the aqueous electrolyte glass*: $LiCl.4D_2O$, manuscript in preparation.
336 N. T. Skipper, A. K. Soper, J. D. C. McConnell and K. Refson, *Chem. Phys. Lett*., 1990, **166**, 141.
337 N. T. Skipper, A. K. Soper and J. D. C. McConnell, *J. Chem. Phys*., 1991, **94**, 5751.
338 N. T. Skipper, A. K. Soper and M. V. Smalley, *J. Phys. Chem*., 1994, **98**, 942.
339 N. T. Skipper, M. V. Smalley, G. D. Williams, A. K. Soper and G. H. Thompson, *J. Phys. Chem*., 1995, **99**, 14 201.